OPTIMIZING YIELD WITH AGRICULTURAL CLIMATE AND WEATHER FORECASTS

A Thesis
Presented to
The Academic Faculty

by

Emily Hall Christ

In Partial Fulfillment
of the Requirements for the Degree
Doctor of Philosophy in the
School of Earth and Atmospheric Sciences

Georgia Institute of Technology
May 2016

OPTIMIZING YIELD WITH AGRICULTURAL CLIMATE AND WEATHER FORECASTS

Approved by:

Dr. Peter J. Webster, Advisor
School of Earth and Atmospheric Sciences
Georgia Institute of Technology

Dr. Guy D. Collins
College of Agriculture and Life Sciences
North Carolina State University

Dr. Judith A. Curry
School of Earth and Atmospheric Sciences
Georgia Institute of Technology

Dr. George Vellidis
College of Agricultural and Environmental Sciences
The University of Georgia

Dr. Robert X. Black
School of Earth and Atmospheric Sciences
Georgia Institute of Technology

Dr. Brenda V. Ortiz
College of Agriculture
Auburn University

Dr. Yi Deng
School of Earth and Atmospheric Sciences
Georgia Institute of Technology

Date Approved: February 9, 2016

To my Lord: Father, Son and Holy Spirit. If I have ever taken a leap of faith, this work has been it. My prayer is that it can be used as a tool for good in the world.

ACKNOWLEDGMENTS

There are so many I wish to acknowledge for supporting me, loving me and talking me down from all those ledges I encountered along the way. First of all, I would like to thank my Maker and Creator for giving me life, directing my path, being my friend and saving me. I wish to thank my husband Joey Christ who is my best friend and has been my rock and my continual support through this process and in every area of life. Special thanks to my parents Ron and Pam Hall who have always loved me and encouraged me to dream big dreams and follow my heart. I am grateful for my friends and family who prayed for me and encouraged me along the way including Missy McNatt, Page Benson and Leslie Harbison among others. I am especially indebted to my grandparents, James and Mildred Hammond, and my great-grandmother, Emily Hammond, who introduced me to the art of growing things and had a beautiful garden every year, no matter what.

I would also like to acknowledge all of those who taught, advised, guided, and ushered me along this journey. I am indebted to Dr. Peter Webster for accepting me into his research group and advising me. Special thanks to all the members of his research group, past and present, including Dr. Violeta Toma, Sebastian Ortega, Dr. Fernando Hirata, Dr. James Belanger, and Dr. Hai-Ru Chang, as well as the members of my comprehensive examination committee (Dr. Judith Curry, Dr. Robert Black, Dr. Yi Deng, Dr. Guy Collins, Dr. George Vellidis, and Dr. Brenda Ortiz) for helpful comments and suggestions. I am indebted to Dr. Kater Hake, Dr. Ed Barnes, Dr. John Snider, Dr. Derrick Oosterhuis, Dr. Daryl Chastain and Dr. Seth Byrd for valuable comments

concerning the applicability of this research to the agriculture industry. I would also like to thank Calvin Perry and others at Stripling Irrigation Research Park who organized and participated in the field experiments included in this thesis as well as the EAS and Cotton, Incorporated administrative staff for all their assistance along the way. I am obliged to Cotton, Incorporated for supporting this research and to the European Centre for Medium-Range Weather Forecasts (ECMWF) for providing forecast data for this research.

TABLE OF CONTENTS

LIST OF TABLES

LIST OF FIGURES

LIST OF SYMBOLS

a	hit
b	false alarm
c	miss
$Cost_{event}$	cost of taking action to protect by irrigation
d	correct rejection
e	vapor pressure in hPa
e_a	mean hourly vapor pressure in kPa
EM	hourly forecast canopy temperature ensemble mean for a given lead day in ˚C
$Events_{July}$	ave no of heat stress events assumed to occur within July
$Events_{Aug\_Sep}$	ave no of heat stress events assumed to occur within Aug or Sept
L_{event}	estimated cost of loss per heat stress event in $\$ha^{-1}$
$Loss_{Aug\_Sep\_event}$	losses per event in August and September in $\$ha^{-1}$
$Loss_{July\_event}$	losses per event in July in $\$ha^{-1}$
MB	hourly mean bias for a given lead day (10 total) in ˚C
obs	hourly observed canopy temperature in ˚C
P_{adj}	adjusted precipitation forecast
P_{cotton}	expected sale price of cotton for the year in consideration in $kgha^{-1}$
P_{fcst}	forecast precipitation
Pr_{fcst}	forecast probability
R^2	r-squared value
S	mean hourly solar radiation in Wm^{-2}
T_a	measured mean hourly ambient environmental air temperature in ˚C
$Tc_{daytime}$	model estimated hourly canopy temperature in ˚C during the day

$Tc_{nighttime}$	model estimated hourly canopy temperature in ˚C during the night
$Tc_{daytime,GA}$	model estimated hourly canopy temperature in ˚C, night in GA
$Tc_{nighttime,GA}$	model estimated hourly canopy temperature in ˚C, day in GA
Tc_{24_hour}	model estimated hourly canopy temperature in ˚C
T_d	dewpoint temperature in ˚C
U	mean hourly wind speed in ms^{-1}
$VarCost_{irrig}$	variable cost of irrigation in \$ $ha^{-1}cm^{-1}$
VPD	mean hourly measured vapor pressure deficit in kPa
Wt_{Aug_Sep}	weighting applied during August and September, 0.25
Wt_{July}	weighting applied during July, 0.75
$Yield_{category}$	represents low, intermediate or high yield losses, by category

LIST OF ABBREVIATIONS

ANOVA	Analysis of Variance
AZMET	Arizona Meteorological Network
B	Bias
CISSHY	Cotton Irrigation Schedule Suggested for High Yields
CW	Correct Warning
DMO	Direct Model Output
DSSAT	Decision Support Technology for Agrotechnology Transfer
ECWMF	European Centre for Medium-Range Weather Forecasts
EPS	Ensemble Prediction System
FAR	False Alarm Ratio
GAEMN	Georgia Automated Environmental Monitoring Network
GDP	Gross Domestic Product
HR	Hit Rate
ME	Missed Event
NCDC	National Climatic Data Center
NWP	Numerical Weather Prediction
ROC	Relative Operating Characteristic
SIRP	Stripling Irrigation Research Park
TKW	Thermal Kinetic Window
UGA	the University of Georgia
UN	United Nations

SUMMARY

Weather affects agriculture more than any other variable. For centuries, growers had to depend upon small bits and pieces of local climatological data collected and passed down in almanacs. Over the last 100 years, however, scientists have developed complex Numerical Weather Prediction (NWP) models that are able to forecast weather with increasing accuracy. The objective of this work was to use a probabilistic NWP model (the European Centre for Medium-Range Weather Forecasts (ECMWF) Ensemble Prediction System (EPS)) as a component to couple with agricultural decision-making tools and models. First, customized ECMWF EPS forecasts were used as an irrigation scheduling aid for a field trial. Next, the CROPGRO Cotton Model was used to simulate the field experiment as well as an additional irrigation scheduling strategy. Finally, a cotton canopy temperature model was developed and coupled with customized ECMWF EPS forecasts to generate hourly canopy temperature forecasts. These forecasts were used to create a heat stress warning system. Results from the field trial indicate that using precipitation forecasts to schedule irrigation could provide a convenient alternative relative to a standard method. Results from the simulated field trial suggest using precipitation forecasts issued on the day of irrigation could be more efficient than using forecasts issued one to two days prior. Last, results from the heat stress project indicate forecasts were skillful to 10 days, allowing enough time for growers to protect crops if needed. In light of the above, implications for the agricultural community could be significant. Coupled atmospheric-agricultural models have the ability to put weather forecasts in terms producers can understand and can quickly use to make strategic on-farm decisions, therefore, possessing the potential to make a large positive global impact.

CHAPTER 1

INTRODUCTION

According to the United States Census Bureau website (www.census.gov), the world population has grown to over 7 billion. Estimates by the United Nations (UN) suggest it will grow to 8.9 billion by 2050 and further to 9.2 billion by 2075 (UN Dept of Economic and Social Affairs 2004). In order to sustain the increasing population, global food demand will increase as well, with estimates ranging from a 60% increase (Pfister et al. 2011) up to near a 100% increase and more (Tilman et al. 2011) by 2050. The increases in demand will be further bolstered by the projected improving economic conditions in developing countries, since it has been demonstrated that per capita food consumption increases as per capita Gross Domestic Product (GDP) increases (Tilman et al. 2011).

Whether or not the agricultural community will be able to keep up with this rising demand will depend upon the trajectory along which global agriculture develops (Tilman et al. 2011). If the agricultural community develops in a more sustainable way, projections suggest that, indeed, there will be enough food and water for the world population (Pfister et al. 2011). However, this will require a concentrated effort among the world's scientists, agriculturists and leaders.

The ideas presented in this thesis are an attempt to aid the agriculture industry in becoming more efficient, resilient and sustainable by translating weather forecasts into tools growers can use when making critical operational decisions. This work includes research and experimentation concerning the use of precipitation forecasts as irrigation scheduling aids, the inclusion of precipitation forecasts into a crop model, and, finally, the development and coupling of a heat stress model for cotton with a global weather forecast model. The research documented in this work is diverse and demonstrates the

wide area of application available for the atmospheric sciences with respect to the agriculture industry.

Thesis Outline

This thesis contains five chapters including three research projects (included in Chapters 2 through 4), an Introduction (Chapter 1) and Conclusion (Chapter 5). Using precipitation forecasts as an irrigation scheduling aid for cotton is explored in Chapter 2. This work has been published in the *Journal of Cotton Science* (Christ et al. 2015a). Chapter 3 discusses the use of the CROPGRO cotton model to simulate the experiment conducted in Chapter 2. Furthermore, it also includes the analysis and comparison of an additional forecast strategy along with those analyzed in the field experiment. Chapter 4 discusses the development of a cotton canopy temperature model and its subsequent coupling with the European Centre for Medium-Range Weather Forecasts (ECMWF) Ensemble Prediction System (EPS) to produce short-term heat stress forecasts for cotton. In addition, a heat stress warning system is developed as a tool to deliver heat stress forecast information in a quick and easy to understand manner. An example is presented identifying a way for growers to use probabilistic forecast information to determine when it is economically responsible to protect against heat stress. This work has been submitted to the *Agronomy Journal* for publication (Christ et al. 2015b).

CHAPTER 2

USING PRECIPITATION FORECASTS TO IRRIGATE COTTON

Recent droughts throughout the country and the continuing water disputes among the states of Georgia, Alabama and Florida have made agricultural producers more aware of the importance of managing irrigation systems efficiently. Some southeastern states are beginning to consider laws that will require monitoring and regulation of water used for irrigation. In fact, Georgia recently suspended issuing irrigation permits in some areas to try and limit the amount of water used in irrigation (Hollis 2013).

Even in southwest Georgia, which receives on average 59.06 cm (23.25 in) of rain during the growing season (April through October), irrigation can significantly impact crop yields. Studies have shown there can be large differences between dry-land cotton (*Gossypium hirsutum* L.) production and irrigated yield. For example, (Farahani and Munk 2012) point out that if sufficient rainfall fails to occur at critical times during the growth cycle of cotton (during the reproductive stages, from floral budding to peak bloom), yield can be less than half that of irrigated fields. On the other hand, irrigation is expensive both in variable costs (which includes expenditures for moving the pivot, labor and repairs, as well as maintenance on the motor, pump and pivot, estimated at $11.67/ha-cm ($12.00/acre-in) in 2013 and fixed costs (which include depreciation, interest and insurance on machinery, equipment and irrigation, estimated at $308.88/ha ($125.00/acre) in 2013) (Shurley and Smith 2013).

Many different irrigation scheduling tools are available for producers, some of which include the input of current weather data from nearby stations (Leib et al. 2012). Most published literature concentrating on weather occurring during the growing season emphasizes the role of large-scale patterns on crop production (Baigorria et al. 2008; Hansen et al. 1998; Hansen et al. 2001; Paz et al. 2012) and not on the effects of using

short-term weather forecasts for management decisions. Although using seasonal weather forecasts for agricultural decision making (e.g. crop and variety decisions) is promising (Crane et al. 2010), the use of more reliable short term forecasts may have substantial benefits for producers as well. In this experiment, the use of probabilistic forecasts (explained in detail later) is highlighted, allowing a way to optimize irrigation by predicting set thresholds of precipitation rather than merely predicting the probability that measurable precipitation will be observed. The objective of this experiment was to compare the yield, water use and irrigation costs associated with treatments irrigated according to recommendations derived from two short-term precipitation forecasts. Each forecast is also analyzed with respect to performance.

Check-book Method

In this study, using precipitation forecasts to schedule irrigation is compared to an accepted irrigation practice referred to as the "check-book" method. The check-book method is a straightforward scheduling aid (University of Georgia Cooperative Extension/ College of Agricultural and Environmental Sciences 2014) and has proven to be a simple and effective way to promote high yields.

To follow the method, producers keep a record of observed rainfall and subtract the observed amount from the total amount of irrigation recommended by the Cotton Irrigation Schedule Suggested for High Yields (University of Georgia Cooperative Extension/ College of Agricultural and Environmental Sciences 2014) provided in Table 2.1. However, there are caveats to the rule. If an intense, quick rainfall occurs on the field in which runoff is assessed qualitatively by the producer as being high, then the total amount of rainfall in that event may not be subtracted from the recommended amount of irrigation for the time period. Also, if rainfall occurs in the midst of several hot, dry days, then the event would not be subtracted from the recommended amount, if the producer observes the ground to be relatively dry at the time of planned irrigation.

During experimentation, the Check-book Treatment was irrigated according to this method.

Table 2.1. Cotton Irrigation Schedule Suggested for High Yields and Twice Per Week Application Rates (University of Georgia Cooperative Extension/ College of Agricultural and Environmental Sciences 2014)

Crop Stage	mm/week	mm/application
Week beginning at 1st bloom	**25.4**	**12.7**
2nd week after 1st bloom	**38.1**	**19.0**
3rd week after 1st bloom	**50.8**	**25.4**
4th week after 1st bloom	**50.8**	**25.4**
5th week after 1st bloom	**38.1**	**19.0**
6th week after 1st bloom	**38.1**	**19.0**
7th week to 1st open boll	**25.4**	**12.7**

European Centre for Medium-Range Weather Forecasts (ECMWF) Ensemble Prediction System (EPS) Probabilistic Precipitation Forecasts

The ECMWF EPS generates probabilistic precipitation forecasts. These forecasts were adjusted and used to irrigate the Bias-Adjusted ECMWF EPS Treatment (see Materials and Methods.) The ECMWF EPS consists of a global atmospheric general circulation model, a data assimilation system, a land surface model, an ocean wave

model, and an ensemble forecasting system. The horizontal resolution of the model is 0.25° (approximately 27 km) (Persson 2011). The model divides the vertical component of the atmosphere into 91 layers covering 64 km at up to 0.1 hPa resolution in the planetary boundary layer, decreasing upward into the stratosphere and lower mesosphere (British Atmospheric Data Centre 2015).

In contrast to deterministic forecasts, which provide one model result per grid point, the ECMWF EPS produces multiple model outcomes per grid point that are intended to compensate more adequately for initial analysis and model error. Forecasts such as these are designed to provide a measure of the forecast uncertainty and probability from which alternative scenarios and strategies can be developed. The ECMWF EPS generates a total of 51 forecasts (ensemble members) for each time step, consisting of the control forecast (the unperturbed model run, which is also run at a finer resolution) in addition to 50 forecasts produced from perturbed model states. These perturbed forecasts are used to represent initial analysis error (by perturbing the initial analysis) and model error (by using stochastic processes to represent errors in model physics). The probability of occurrence of an event (i.e., rainfall above or below some threshold) can be characterized by the number of ensemble members predicting the event divided by the total number of members (Persson 2011).

Weather.com Forecasts

The Weather Channel®'s mobile app (http://www.weather.com/apps) was chosen as the second forecast option due to its accessibility and popularity. Due to its close proximity to Stripling Irrigation Research Park (SIRP), Camilla, GA was set as the forecast location in the app. Unlike the ECMWF EPS, probabilities for precipitation issued by weather.com were not determined based upon a set threshold for an amount of precipitation, but rather upon the probability of receiving any measurable rainfall (considered to be greater than 0.254 mm [0.01 in]).

Materials and Methods

Experimental Design

Two cotton varieties, PhytoGen® 499 WRF ('PHY 499 WRF', considered to be more drought tolerant) and FiberMax® 1944 GLB2 ('FM 1944 GLB2', considered to be more responsive to water), were planted in a split block design at the University of Georgia's (UGA) SIRP located near Camilla, GA (31° 16′ 48.288" N, -84° 13′ 10.5594" W, 49 m elevation above sea level). The experiment consisted of four irrigation treatments: Rainfed, Check-book, Weather.com, and Bias-Adjusted ECMWF. Other than differences in irrigation, management practices used throughout the season were consistent across treatments.

Each treatment was replicated three times, with each sub-block consisting of two varieties subjected to one of the four irrigation treatments. Rows were 91 cm (36 in) wide and 13.7 m (45 ft) long. Seeds were sown at 3 seeds/30.5 cm (3 seeds/ft) with a Monosem® (Edwardsville, KS) vacuum planter on 7 May 2014 in Lucy loamy sand, characterized as being very deep, well drained, and moderately permeable. Irrigation was initiated with squaring, which began the week of 8 June 2014 and ceased upon boll opening, which began 30 August 2014. A 3-Span Valley® (Valley, NE) Linear Endfeed 8000 with Nelson® (Walla Walla, WA) S3000 Spinner sprinklers regulated at low pressure was used to apply irrigation. The drop hose was held constantly at approximately 2.03 m (80 in) from the ground to the base of the sprinkler. A two-row 9930 John Deere® spindle harvester with bagging attachments was used to harvest the crop on 6 October 2014. Seed cotton was ginned through the UGA Microgin.

For the Rainfed Treatment, cotton only received water during the limited number of rainfall events that occurred throughout the 2014 growing season. For the other three treatments, irrigation schedules and amounts were based upon values derived from the Cotton Irrigation Schedule Suggested for High Yields (CISSHY) found in Table 2.1

(University of Georgia Cooperative Extension/ College of Agricultural and Environmental Sciences 2014). This table recommends irrigation based upon cotton crop stage and commonly is followed when applying the check-book method of irrigation.

Irrigation was scheduled twice per week on Mondays or Tuesdays for the first application and Thursdays or Fridays for the second, depending upon time and availability at SIRP. Irrigation was applied to all treatments the same day. Irrigation decisions pertaining to the Bias-Adjusted ECMWF Treatment and the Weather.com Treatment were made twice per week on Sunday and Wednesday evenings after observing the forecasts. Irrigation decisions for the Check-book Treatment were made twice per week, the evening before scheduled irrigation. However, if rainfall occurred overnight, adjustments were made on the morning of irrigation. During the experiment, 1.27 cm (0.5 in) of water was not applied as prescribed to the two forecast treatments and should be noted as experimental error. The errors occurred during the same irrigation applications for both treatments.

Forecasts are available from the ECMWF EPS twice daily at 0Z and 12Z (8 pm and 8 am EDT). However, many producers are constrained by pivot size and speed to make irrigation decisions only two to three times per week. During this experiment, forecasts using the ECMWF EPS model data were issued twice per week, on Sunday and Wednesday evenings at 1700 (5 pm) EDT and communicated by e-mail. The Sunday evening forecasts included precipitation forecast data from the Sunday 0Z (8 pm EDT Saturday) ECMWF EPS model run, whereas the Wednesday evening forecasts included precipitation forecast data from the Wednesday 0Z (8 pm EDT Tuesday) model run. Forecasts from weather.com were downloaded twice per week on Sunday and Wednesday evenings at 1700 (5 pm) EDT.

Bias Adjustments

Numerical Weather Prediction (NWP) models frequently display bias with respect to forecasts (Danforth et al. 2007). In an effort to reduce bias in the ECMWF EPS model forecasts, a statistical technique known as quantile-to-quantile (q-to-q) mapping (Hopson and Webster 2010; Shrestha et al. 2014; Webster et al. 2011) was applied. For this experiment, q-to-q mapping was performed on each ensemble member to generate a corrected ensemble member forecast. As applied here, the q-to-q technique requires the creation of two cumulative distribution functions (cdfs). One cdf consists of past forecast data the other of past observations for the forecast location (or area) in question. ECMWF model hindcasts (re-forecasts for previous years generated once per week using the current version of the model) were used to represent past model forecasts, and observations from the Georgia Automated Environmental Monitoring Network (GAEMN, www.georgiaweather.net) were used to represent past observations. (The process of developing the hindcast and observation cdfs is further explained in the next section.) The q-to-q technique assigns each ensemble member forecast to a quantile on the hindcast cdf. The next step takes the assigned quantile and maps it to a new, "corrected" forecast value on the observation cdf. This bias-correction process is presented in Figure 2.1.

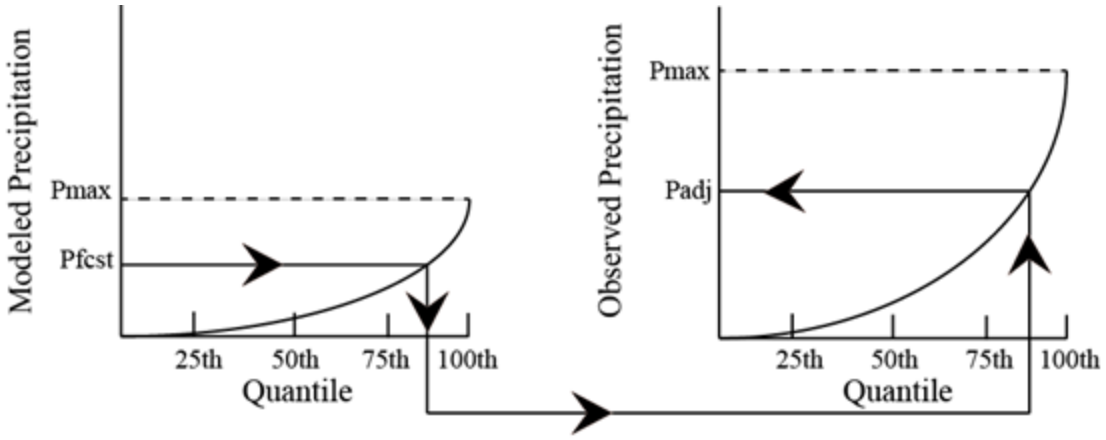

Figure 2.1: The q-to-q Correction System. Both modeled and observed precipitation are binned into quantiles. Precipitation is represented on the y-axis. The modeled precipitation is mapped onto the observed precipitation fields by setting respective modeled quantiles to observed quantiles. In the figure, the forecast precipitation (P_{fcst}) of the 85th quantile is set to the observed precipitation (P_{adj}) of the 85th quantile. (Hopson and Webster 2010)

Hindcasts and Observations

In an effort to measure model performance, the ECMWF runs the most current EPS with fewer ensemble members (5 instead of 51) using past data to initialize the run. These are referred to as hindcasts, and they are run for the entire globe once per week for that calendar day over the previous 18 yrs. For this experiment, hindcasts taken from a sampling of grid points near GAEMN stations in the vicinity of SIRP from 1 May 2013 through 15 August 2013 were used to represent the past model forecasts in a cumulative distribution function (cdf) to be used in the q-to-q correction process. For each chosen station, hindcasts from the nearest five grid points were included in the cdf. Cumulative distribution functions were created for each lead day generated by the model. This made it possible to apply q-to-q corrections specifically for every forecast lead day.

Hindcasts from grid points near the following GAEMN stations were included in the model corrections: Camilla (located at SIRP), Tifton, Dawson, Cordele, Newton, Moultrie, Attapulgus and Dixie. The hindcast cdf is represented by the plot on the left-hand side of Figure 2.1, with modeled precipitation represented on the y-axis. Observations taken during the time period beginning 1 May and running through mid-August over the previous 18 yrs from the above GAEMN stations were used to generate a cdf of observations. The observation cdf is represented by the plot on the right-hand side of Figure 2.1, with observed precipitation represented on the y-axis. Figure 2.2 shows the hindcasts for lead day one plotted versus the historical observations, illustrating a tendency (bias) to under-predict precipitation for larger observed values. Therefore, the q-to-q corrections helped improve the model's tendency to under-predict precipitation by mapping it to larger values for the same quantile on the observed cdf.

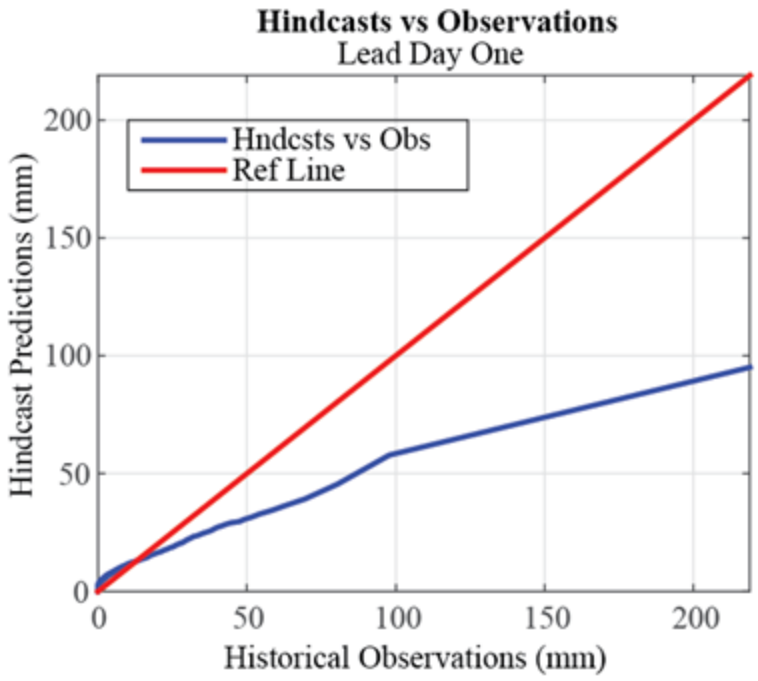

Figure 2.2: Lead Day One Plot of Hindcasts vs Historical Observations. Hindcasts tend to over-predict precipitation in the lower values while under-predicting in the upper values.

Bias-adjusted Forecasts

The above correction technique was applied to each ensemble member generated by the ECMWF EPS precipitation forecasts, creating 51 Bias-Adjusted ECMWF EPS forecasts for each chosen grid point. Grid points chosen for the forecasts included data from an approximate 1° latitude-longitude box surrounding SIRP. To summarize, there were 51 ensemble members produced at each grid point and 25 grid points chosen for analysis. The forecast probabilities issued were the percent number of ensemble members that predicted at least a threshold value of precipitation would occur as described in Equations 2.1 and 2.2, below. These Bias-Adjusted ECMWF EPS forecast probabilities were then communicated twice per week via e-mail. An example forecast is shown in Figure 2.3.

$$Total\ No\ of\ Ens\ Members = 51\ \frac{ens\ members}{grid\ point} * 25\ grid\ points = 1275\ Total\ Ens\ Members \quad (2.1)$$

$$Forecast\ Probability = \frac{number\ of\ ensemble\ members \geq threshold}{total\ number\ of\ ensemble\ members} \quad (2.2)$$

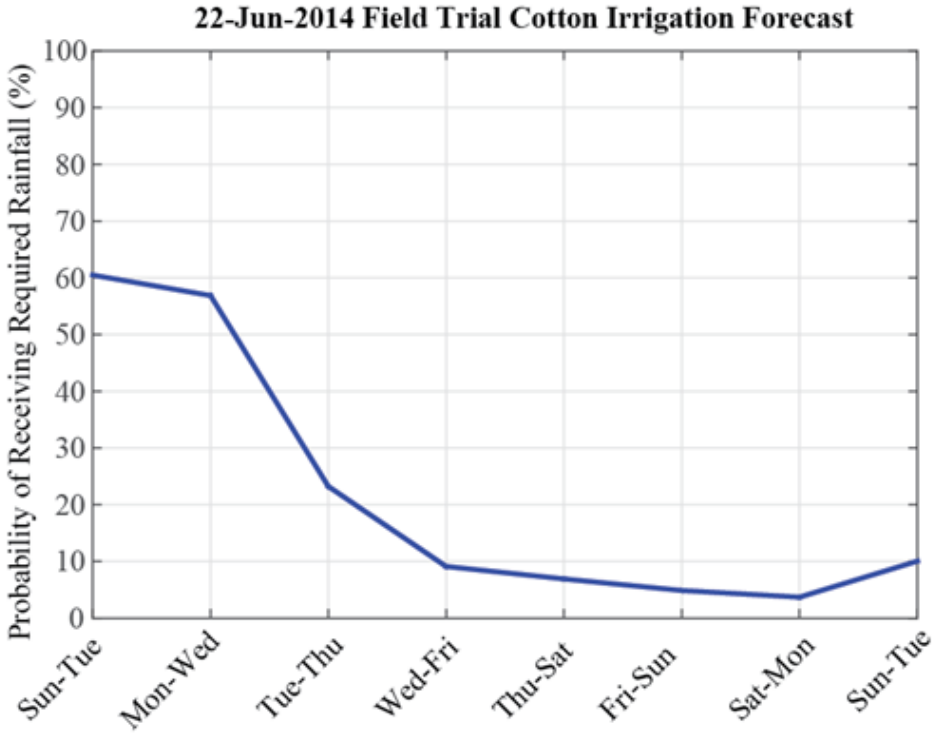

Figure 2.3: 22 June 2014 Bias-Adjusted ECMWF Treatment Forecast.

Precipitation Thresholds

Precipitation thresholds were developed for the Bias-Adjusted ECMWF Treatment so that forecast probabilities could be calculated for each time period. Irrigation began upon squaring, and from the onset of irrigation through the first week of bloom, the forecast thresholds were set at 12.7 mm (0.5 in). This threshold matched the CISSHY found in the 2014 UGA Cotton Production Guide provided in Table 2.1. Following the first week of bloom and for the remainder of season, the forecast thresholds were set at 2.54 mm (0.1 in), 5.08 mm (0.2 in), 7.62 mm (0.3 in), and 10.2 (0.4 in) for each forecast. If the probability of receiving one of the lower precipitation thresholds exceeded the probability limit, then it was subtracted from the total amount recommended by the CISSHY.

Probability Limit

A probability limit was set for the experiment so that any forecast exceeding it would trigger cancellation of the planned irrigation. This limit was set somewhat liberally at 60% to compensate for conservative model estimates of the predominantly convective nature of precipitation occurring in Southwest Georgia during the growing season (Tiedtke 1989). The decision to irrigate cotton included in the Bias-Adjusted ECMWF Treatment was based upon a 60% probability of exceeding the set threshold amount of precipitation occurring between Monday and Wednesday (for the Sunday-issued forecasts) and Thursday through Sunday (for the Wednesday-issued forecasts). Cotton included in the Bias-Adjusted ECWMF Treatment was irrigated according to the CISSHY, provided in Table 2.1, when forecast probabilities were less than 60%.

The threshold for irrigation was set at 60% for the weather.com forecasts as well. If there was a 60% chance or more for precipitation during the Monday through Wednesday time period (Sunday forecast) or Thursday through Sunday time period (Wednesday forecast), then irrigation was not applied. Cotton included in the

Weather.com Treatment was irrigated according to the CISSHY, provided in Table 2.1, when forecast probabilities were less than 60%.

Forecast Verification

There are many different ways to verify and compare weather forecasts. One common method is by compiling a 2-X-2 contingency table (Nurmi 2003). Contingency tables separate forecasts into four distinct categories as shown in Table 2.2: hits (a), false alarms (b), misses (c), and correct rejections (d). Although categorically different, the two forecasts used in this experiment were converted into simple binary (or yes/no) forecasts using a defined probability threshold.

Table 2.2. 2-X-2 Contingency Table. Contingency tables separate forecasts into four distinct categories (a-d). The variables generated from these categories are used to evaluate forecast performance.

	Event Observed		
Event Forecast	**Yes**	**No**	**Marginal Total**
Yes	**a^z**	**b^y**	**$(a+b)^x$**
No	**c^w**	**d^v**	**$(c+d)^u$**
Marginal Total	**$(a+c)^t$**	**$(b+d)^s$**	**$n = (a+b+c+d)^r$**

[z] referred to as a Hit
[y] referred to as a False Alarm
[x] total number of times the event was forecast
[w] referred to as a Miss
[v] referred to as a Correct Rejection
[u] total number of times the event was not forecast
[t] total number of times the event was observed
[s] total number of time the event was not observed
[r] total number of forecasts in the season

Binary Analysis

Bias-Adjusted ECMWF EPS forecasts were grouped into the "yes" category if the probability of exceeding one of the set threshold precipitation levels exceeded the probability limit (60%); otherwise, the forecasts were grouped into the "no" category. Weather.com forecasts were classified into the yes category if the probability limit was exceeded. Observations were included in the no category for the Bias-Adjusted ECWMF EPS forecasts when the forecasted precipitation threshold was not observed; likewise, forecasts were grouped into the yes category when the threshold was met or exceeded. Similarly for the weather.com forecasts, observations were included in the no category when the recommended amount of precipitation for the time period was not observed and were classified in the yes category when the recommended amount of precipitation for the time period was observed.

Categorical Analysis

Several useful variables can be defined based upon combinations and ratios of the different categories contained in a contingency table. These variables are commonly used in the atmospheric sciences to verify and compare forecast performance. In particular, the Hit Rate (HR or Probability of Detection, POD, defined below in Equation 2.3) and the False Alarm Ratio (FAR, defined below in Equation 2.4) can be used together to evaluate forecast performance. Calculations of HR and FAR for this experiment are included in Table 2.3 (Nurmi 2003).

Table 2.3. Hit Rate, False Alarm Ratio and Bias Calculated for the Bias-Adjusted ECMWF EPS and weather.com Forecasts. These calculations are used to judge forecast performance

Verification Variable	Bias-Adjusted ECMWF EPS	Weather.com
Hit Rate (HR)	**0.2**	**0**
False Alarm Ratio (FAR)	**0.6**	**1**
Bias (B)	**0.5**	**1.2**

$$HR = a/(a+c) \tag{2.3}$$

$$FAR = b/(a+b) \tag{2.4}$$

The HR measures the proportion of observed events that were correctly forecast, whereas the FAR measures the proportion of events incorrectly forecast. Values for HR range between 0 and 1, with 1 being a perfect score, whereas values for FAR vary between 0 and 1, with 0 being a perfect score.

The Bias (B) is also included in Table 2.3 and defined in Equation 2.5. Although Bias is not an indicator of accuracy, it is useful in evaluating how a system behaves with respect to forecasting a given event (Nurmi 2003). Bias values greater than 1 indicate the system over-predicts an event, bias values less than 1 indicate the system tends to under-predict, and bias values equal to 1 indicate the system is unbiased.

$$B = (a+b)/(a+c) \tag{2.5}$$

Statistical Analysis

Statistical analysis was performed in MATLAB (R2014b) using two-way analysis of variance (ANOVA) followed by a multiple comparison of means.

Results and Discussion

The objective of this experiment was to demonstrate the potential of using precipitation forecasts to schedule irrigation. The ECMWF EPS is introduced, with the option to use its forecast data to predict the probability of exceeding predetermined threshold values of precipitation. Bias adjustments and forecast data from the surrounding area are included in the analysis to de-emphasize any sub-grid scale anomalies (such as convective precipitation) occurring at one point that might not be representative of the entire area. It is contrasted with a more common forecast issued by The Weather Channel, which does not provide information pertaining to the amount of rainfall anticipated and is issued for a single location.

Forecast Analysis

Table 2.3 lists the HR and FAR for the Bias-Adjusted ECWMF EPS forecasts and the weather.com forecasts. The Bias-Adjusted ECMWF EPS forecasts out-performed the weather.com forecasts with respect to HR and FAR, although there is room for improvement. It is also interesting to note that the weather.com forecasts did not correctly predict any rainfall events throughout the season, meaning that on the six times the forecast predicted rainfall (13 June, 11 July, 22 July, 25 July, 8 August, and 12 August), none of the events met or exceeded the recommended amount of water for irrigation. Therefore, a producer using these forecasts would have withheld irrigation during time periods in which rainfall either did not occur or the amount of observed was less than the amount recommended.

Q-to-q corrections were applied to the ECMWF EPS forecasts during the experiment in an effort to reduce bias; however, bias remained. Values for B found in Table 2.3 indicate that the Bias-Adjusted ECMWF EPS system tended to under-predict rainfall events, whereas the weather.com forecasts tended to over-predict precipitation. From a producer standpoint, it could be more beneficial to choose a forecast system that, to an extent, tends to under-predict rainfall rather than over-predict, thus protecting against water stress. If this were the case, the Bias-Adjusted ECMWF EPS forecasts would be a better choice both in terms of B and overall forecast performance.

Water Applied

Total water applied for each treatment was calculated by summing all the irrigation applications during the season. Water applied over the course of the season totaled 34.80 cm, 31.93 cm, and 26.67cm for the Bias-Adjusted ECMWF, the Weather.com, and Check-book treatments, respectively. The larger amount of water applied to the Bias-Adjusted ECMWF Treatment reflects the tendency to under-predict rainfall indicated by the values for B calculated in the previous section. Similarly, the smaller amount of water applied to the Weather.com Treatment reflects the tendency for these forecasts to over-predict precipitation.

Yield

Yields from the Bias-Adjusted ECMWF Treatment were the greatest followed by the Weather.com Treatment, the Check-book Treatment, and the Rainfed Treatment, averaging 1796 kg/ha, 1717 kg/ha, 1692 kg/ha and 730 kg/ha, respectively. Because there was no interaction between irrigation method and cultivar, the statistical analyses for the two varieties were combined and are presented in Table 2.4. The results show that yields from the Rainfed Treatment are significantly different (lower) than the irrigated treatments. There is no significant difference among yields of the irrigated treatments

(the Check-book Treatment, the Bias-Adjusted ECWMF Treatment, or the Weather.com Treatment) at a 95% confidence level.

Table 2.4. Statistical Analysis. Two-way analysis of variance (ANOVA) followed by a multiple comparison of means was performed as the statistical analysis. Because there was no interaction between irrigation method and cultivar, the statistical analyses for the two varieties were combined.

Yield Comparison between Treatments		***p*-values[z]**
Check-book Trtmt	**Bias-Adjusted Trtmt**	**4.00E-01**
Check-book Trtmt	**Weather.com Trtmt**	**1.00**
Check-book Trtmt	**Rainfed Trtmt**	**~0**
Bias-Adjusted ECMWF Trtmt	**Weather.com Trtmt**	**6.0E-01**
Bias-Adjusted ECMWF Trtmt	**Rainfed Trtmt**	**~0**
Weather.com Trtmt	**Rainfed Trtmt**	**~0**

[z] *p*-values < 0.05 indicate statistically significant differences in mean yields

The Check-book Treatment was included primarily as a yield comparison for the two forecast treatments. The results of this short study indicate that it might be possible use precipitation forecasts to maintain yield at levels comparable to those one would expect using the check-book method. Therefore, instead of keeping record of past rainfall as with the check-book method, producers could save time by simply looking at the precipitation forecast to schedule irrigation.

Future Work

The creation of a forecast system designed to serve agricultural interests and provide information specifically tailored for the agricultural industry has the potential to make a large positive impact both within and beyond the irrigation sector. To accomplish this, however, work needs to be done to improve the accuracy of ECMWF EPS and weather.com forecasts in southern Georgia and other areas of intense agricultural industry. Work has begun to characterize the ECMWF EPS performance over the southern Georgia region. This work will be key in determining how to improve forecast accuracy. Once the forecasts have been optimized, it would be beneficial to run a series of field trials over a period of several seasons to further study the usefulness of precipitation forecasts with respect to scheduling irrigation.

Additionally, more research needs to be done on the manner and timing in which forecasts are used. There are many different methods producers use to irrigate. The only one explored in this research was the check-book method. Therefore, it would be constructive to use precipitation forecasts in conjunction with additional methods such as the use of sensor systems to see if results could be further optimized.

CHAPTER 3

SIMULATING AND IMPROVING 'USING PRECIPITATION FORECASTS TO IRRIGATE COTTON'

In Chapter 2 (Christ et al. (2015a)), the idea was put forth that growers could use precipitation forecasts as an irrigation scheduling aid to maintain high yields in irrigated cotton (*Gossypium hirsutum* L.). Irrigation was planned twice per week. Therefore, forecasts were issued twice per week strictly on Sunday and Wednesday evenings. Two types of forecasts were provided during the experiment. One was a more common deterministic forecast issued by Weather Channel (www.weather.com). The second was a bias-adjusted forecast using data from the European Centre for Medium-Range Weather Forecasts (ECMWF) Ensemble Prediction System (EPS). These forecasts were used in conjunction with the check-book method (University of Georgia Cooperative Extension/ College of Agricultural and Environmental Sciences 2014) to schedule irrigation during the field experiment. The results showed that the Bias-Adjusted ECMWF EPS forecasts outperformed the forecasts issued by The Weather Channel. The work documented in this chapter is an attempt to determine the feasibility of improving upon the results of the field experiment by simulating the use of Bias-Adjusted ECMWF EPS precipitation forecasts issued on the day of irrigation, referred to as Same-Day Bias-Adjusted ECMWF forecasts.

Decision Support Technology for Agrotechnology Transfer (DSSAT)

The CROPGRO cotton model found in the Decision Technology Support System for Agrotechnology Transfer (DSSAT) Version 4.6 (Hoogenboom et al. 2014) was used to simulate crop growth and yield in this study. It is a software application program containing models for over 28 crops. DSSAT has a modular structure, featuring a main

driver program, a land unit module, and modules for the primary components that make up a land unit in a cropping system. The land unit modules consist of programs written for weather, soil, plant, soil-plant-atmosphere interface, and management components. Once initiated, these components describe the time changes in the soil and plants occurring on a single land unit in response to weather and management. (Jones et al. 2003)

Materials and Methods

Experimental Design

DSSAT Version 4.6 does not output lint yield; therefore, seedcotton yield (the weight of the lint in addition to the seed weight per area harvested) and water use were simulated using the CROPGRO-Cotton Model included in the DSSAT Version 4.6 for the 2014 growing season at the Stripling Irrigation Research Park (SIRP) in Camilla, Georgia. Observed weather including daily maximum temperature, minimum temperature, precipitation and total solar radiation were provided by the Georgia Automated Environmental Monitoring Network (www.georgiaweather.net). The Camilla, Georgia weather station located at SIRP (31.2008 N, -84.29161 E) was used as the source location for weather data input. The planting date (7 May 2014), fertilizer application rates and dates, and tillage dates and implements were simulated as carried out in the field trial. Values for cotton cultivar coefficients, plant spacing, plant population, row width and soil data were taken from Ortiz et al. (2009). Using accurate cultivar coefficients are essential for model performance. The CROPGRO Cotton Model has been thoroughly evaluated using the cultivar coefficients developed for the Delta Pine 458 Boll Guard/ Roundup Ready (DP 458 BG/RR) cotton cultivar in Ortiz et al. (2009).

Treatments

Five irrigation treatments were simulated. The Check-book Treatment, the Weather.com Treatment, the Bias-Adjusted ECWMF Treatment and the Rainfed Treatment were simulated as completed in Chapter 2 (Christ et al. (2015a)). The fifth treatment consisted of using Bias-Adjusted ECMWF forecasts issued the day of irrigation, referred to in this chapter as the Same-Day Bias-Adjusted ECMWF Treatment.

Forecast Verification

Forecast performance was characterized according to Hit Rate (HR), False Alarm Rate (FAR) and Bias (B), all of which can be derived from a contingency table (see Table 2.2). Equations for HR, FAR, and B are provided in Equations 2.3, 2.4, and 2.5. Values for HR and FAR range between 0 and 1.

The HR is the proportion of times an event was forecast and actually observed. The closer the value to one, the better. The FAR is the proportion of times an event was not observed, yet it was forecast. The closer the value to zero, the better. Bias indicates the propensity for the forecast system to under-forecast or over-forecast a given parameter such as precipitation. The closer to one, the better. If the value of B is less than one, then the forecast system tends to under-predict, if the B is greater than one, then the systems tends to over-predict.

Results

Forecast Analysis

Results from the forecast analysis are included in Table 3.1. The Same-Day Bias-Adjusted ECMWF EPS forecasts out-performed the Weather.com and Bias-Adjusted ECMWF EPS forecasts used in the field trial. The Same-Day Bias-Adjusted ECMWF EPS forecasts had a higher HR, a lower FAR and a B closer to one during the 2014

growing season, indicating they were an improvement over the forecasts used in the field trial in all three verification categories.

Table 3.1. Hit Rate (HR), False Alarm Ratio (FAR) and Bias (B) Calculated for the Bias-Adjusted ECMWF EPS and weather.com Forecasts from the Field Trial as well as the Same-Day Bias-Adjusted ECMWF EPS Forecasts Used as an Additional Treatment in the Simulation. These calculations are used to judge forecast performance.

Verification Variable	Bias-Adjusted ECMWF EPS	Weather.com	Same-Day Bias-Adjusted ECMWF EPS
Hit Rate (HR)	**0.2**	**0**	**0.36**
False Alarm Ratio (FAR)	**0.6**	**1**	**0.56**
Bias (B)	**0.5**	**1.2**	**0.81**

Water Applied

The water applied to the Rainfed Treatment, the Check-book Treatment, the Bias-Adjusted ECMWF Treatment and the Weather.com Treatment was simulated as in the field trial. The water applied to the Same-Day Bias-Adjusted ECMWF Treatment was calculated considering the Same-Day Bias-Adjusted ECMWF EPS forecasts. Irrigation applied over the course of the season was 34.8 cm, 26.67 cm, 31.93 cm, and 33 cm for the Bias-Adjusted ECMWF, the Weather.com, the Check-book and the Same-Day Bias-Adjusted ECMWF Treatments, respectively. Using the Same-Day Bias-Adjusted ECMWF EPS forecasts decreased the amount of irrigation water used over the course of the season as compared to the Bias-Adjusted ECMWF forecasts implemented in the field trial.

Yield

Simulated and actual seedcotton yields are provided in Table 3.2. Simulated yields followed the same order from greatest to least as the actual yields. As in the field trial, yields for the Bias-Adjusted ECMWF Treatment were the greatest. However, the simulated results indicate the Same-Day Bias-Adjusted ECMWF Treatment produced slightly lower yield values than the Check-book Treatment, the Weather.com Treatment and the Rainfed Treatment.

Table 3.2. Yield Comparison among Treatments

Treatment	Actual Seedcotton Yield, $kgha^{-1}$	Simulated Seedcotton Yield, $kgha^{-1}$
Rainfed	**2016**	**1902**
Check-book Trtmt	**4280**	**4418**
Weather.com Trtmt	**4436**	**4471**
Bias-Adjusted ECMWF Trtmt	**4660**	**4483**
Same-Day Bias-Adjusted ECMWF Trtmt	**N/A**	**4407**

Discussion

CROPGRO cotton was able to simulate similar yields in magnitude and order to those observed in Christ et al. (2015a). Although the soil and cultivar characteristics used in the simulation were not taken directly from field trial, they were similar enough to produce results in-line with observation. More studies need to be done to determine if the

results are solely a characteristic of this study or if they are repeatable. However, it would be beneficial to determine if crop models could be used to simulate irrigation strategies dependably for producers using soil and cultivar profiles that are similar to a producer's. If so, then crop models could be used more widely in the future along with improved weather forecasts to predict water usage and yield before the season begins.

Future Work

Future work will include additional simulations of field trials conducted under different irrigation scheduling techniques over multiple seasons in various locations. The purpose of the work will be to determine if the crop model is able to simulate yield comparable to actual results. If so, this will allow broader use such as experimentation with original ways in which to incorporate weather forecasts into on-farm managerial strategies.

CHAPTER 4

PREDICTING HEAT STRESS IN COTTON USING PROBABILISTIC CANOPY TEMPERATURE FORECASTS

The effects of high temperature stress on humans have been well documented. Prolonged exposure to elevated temperatures can cause heat stroke, heat exhaustion, heat cramps, premature births, and a range of health risks (Centers for Disease Control and Prevention 2014). These conditions are caused when the body's normal cooling mechanisms of vasodilation and perspiration are overcome, allowing the core body temperature to rise to unhealthy levels. At very high body temperatures, permanent damage can occur to the brain and other vital organs and can even lead to death (Centers for Disease Control and Prevention 2006). The heat wave that engulfed France during a 20 day period in August 2003 made worldwide headlines by claiming over 14,000 lives, and similar scenarios have played out all over the world (Kovats and Hajat 2008). Already this year in May, India experienced a heat wave that took the lives of over 1,000 people (Bhalla 2015). Fortunately, one city in India had put a plan in place to prepare for extreme heat. Ahmedabad's "Heat-Health Action Plan" (Knowlton et al. 2014) uses 7-day probabilistic weather forecasts to forewarn city leaders concerning impending heat waves. These forecasts allowed time to implement mitigatory resources for those in society threatened by heat.

Although somewhat less in the public mind, high temperature stress occurs in plants as well. Plants, similar to humans, have cooling mechanisms for temperature regulation during times of extreme heat. In cotton (*Gossypium hirsutum* L.), cooling is accomplished by opening stomates in the leaves, allowing evaporation to cool the plant when it becomes too warm. This mechanism works quite well, especially in dry climates

where evaporative cooling can be very effective. For example, in Arizona, with air temperatures measuring 49˚C, well-watered cotton plant canopy temperatures were measured at 31˚C compared to canopy temperatures in water stressed fields that reached 40˚C (Hake and Silvertooth 1990). Therefore, as with humans, the natural cooling mechanism in plants can be overcome under certain conditions, causing irreversible damage and even death to the plant.

The effects of high temperature stress on cotton were reviewed in Oosterhuis and Snider (2011). Among these effects are decreased growth rate, decreased photosynthesis, and decreased membrane integrity. High night temperatures have been shown to increase respiration rates, decrease soluble carbohydrate concentrations in source leaves, and increase boll abscission or shedding. Because reproductive development is particularly sensitive to high temperature stress, it has also been linked to lower yield. More specifically, decreased yield due to high temperatures has been tied to fewer bolls per plant and smaller boll size (Snider and Oosterhuis 2015). Reddy el al. (1992) attributes decreased boll mass to higher rates of boll abscission in accord with subsequent studies (Lokhande and Reddy, 2014; Reddy et al., 1999; Zhao et al., 2005). Pettigrew (2008) associates smaller boll size caused by high temperatures to a decreased number of seeds per boll, which likely limits fertilization efficiency (reviewed in Oosterhuis and Snider, 2011; Snider and Oosterhuis, 2011, 2012).

Defining Heat Stress

Mahan and Upchurch (1988) and Upchurch and Mahan (1988) suggest that plants have the ability to maintain a normative temperature. Plants have the ability to do this in a limited manner such that environmental temperatures less than the optimum (for cotton, 27 ± 2˚C) are set by the environment. These studies suggest three constraints on maintenance of the normative temperature: (1) sufficient energy influx to raise plant temperature to the normative value, (2) a sufficient water supply for transpiration, and (3)

humidity levels low enough to allow for evaporative cooling. During periods when ambient temperatures exceed the optimum value, plants abiding the three constraints can maintain canopy temperatures less than the environment and within 2°C of the ideal. This maintenance was accomplished by transpirational cooling.

Transpiration effects also can be present at night. For example, Upchurch and Mahan (1988) reported plant temperatures within 2°C of the normative temperature while the environmental temperatures were found to be as high as 39°C during the nighttime hours. This suggests that plants are able to regulate a constant ideal temperature for the plant throughout the diurnal cycle.

The normative temperature has been tied to the Thermal Kinetic Window (TKW) for enzyme activity. The TKW has been defined as the range of plant temperatures at which the Michaelis constant, Km, of an important metabolic enzyme is at or below 200% of the minimum observed value (Mahan et al. 1990). Due to its link to efficient enzyme function, the TKW correlates strongly with optimal temperatures for general metabolism and growth for various species (Burke 1990; Burke et al. 1988). The TKW for cotton has been determined to be between 23.5 and 32°C (Burke et al. 1988). We define time periods of heat stress to include hours during the diurnal cycle in which the canopy temperature exceeds the upper limit of the TKW.

Rationale

Creating advisories for cotton that are similar to those used to warn humans of impending periods of heat stress has the advantage of informing producers of damaging conditions ahead of time. The ability to predict heat stress several days in advance would provide growers the opportunity to put protective measures in place before damage is done. In this work, a cotton canopy temperature model is developed and coupled with an atmospheric predictive model, producing canopy temperature forecasts out to 10 days. Subsequently, a heat stress warning system is developed and analyzed. The warning

system is designed to provide information pertaining to the probability of heat stress occurring during the forecast period. Additionally, a short economic analysis is included that estimates the cost to protect against heat stress based upon forecast probability and the possible losses incurred. The economic analysis is intended to be viewed as an example of how probabilistic forecasts can be used to help growers make financial decisions pertaining to weather-related risks.

Materials and Methods

Mean hourly average canopy temperatures were recorded for well-watered cotton plants during 2013 and 2014 at the University of Georgia's (UGA's) Stripling Irrigation Research Park (SIRP) located near Camilla, Georgia (31° 16' 48.288" N, -84° 13' 10.5594" W, 49 m elevation above sea level). Canopy temperature measurements were recorded from 5 July 2013 through 23 August 2013 and 7 July 2014 through 1 October 2014 using SmartCrop® infrared sensors. Sensors were arranged and measured according to Snider et al. (2015). Dates that were excluded from analysis during the 2013 and 2014 seasons during which sensors were inoperative or pesticides were being applied are provided in Table 4.1. Data from the Georgia Automated Environmental Monitoring Network (GAEMN, www.georgiaweather.net) collected at the Camilla, Georgia field site were used to model real-time hourly canopy temperature. The following three sections describe the methods used to analyze and develop several canopy temperature models.

Table 4.1. Dates Excluded from Analysis. The dates listed were excluded due to pesticide applications or sensor failure.

Year	Month		
	July	***August***	***September***
2013	8, 10, 18-25	6-7, 14-17	---
2014	16, 19-22, 31	8-14, 29-30	1-8

Brown and Zeiher Model

Brown and Zeiher (1998) developed cotton canopy temperature models that accounted for ambient air temperature, vapor pressure and vapor pressure deficit. The models were developed based upon observations obtained from the AZMET (The Arizona Meteorological Network, http://ag.arizona.edu/azmet) and field measurements of canopy temperature. One model was used to predict daytime canopy temperatures, while a second version was used to predict nighttime canopy temperatures as expressed in Equations 4.1 and 4.2 below:

$$Tc_{daytime} = 0.53 + T_a - 1.43 * VPD \quad (4.1)$$

$$Tc_{nighttime} = -5.93 + T_a + 1.95 * e_a \quad (4.2)$$

Here, T_c is the hourly canopy temperature estimated by the model in ˚C, T_a is the measured mean hourly ambient environmental air temperature in ˚C, *VPD* is the mean hourly measured vapor pressure deficit in kPa, and e_a is the mean hourly vapor pressure in kPa. The daytime equation was used for time periods after sunrise and before sunset, while the nighttime equation was used between sunrise and sunset (United States Naval

Observatory Astronomical Applications Department, http://aa.usno.navy.mil). These equations were used to calculate modeled values for canopy temperature for Camilla, Georgia during the time periods in 2013 and 2014 in which canopy temperature data were recorded.

The Daytime and Nighttime Georgia Models

Daytime and nighttime canopy temperatures were simulated during the 2014 season using the same variables as in the Brown and Zeiher (1998) model (air temperature and vapor pressure deficit (day) and air temperature and vapor pressure (night)). The models were developed using multiple regression in MATLAB (R2014b) and data collected during the 2013 season. They are provided in Equations 4.3 and 4.4.

$$Tc_{daytime,GA} = -3.5529 + 1.1728 * T_a - 1.2001 * VPD \quad (4.3)$$

$$Tc_{nighttime,GA} = 4.2153 + 0.74375 * T_a + 0.67888 * e_a \quad (4.4)$$

These equations were used to calculate modeled values for canopy temperature for Camilla, Georgia during the time periods in 2013 and 2014 in which canopy temperature data were recorded.

The 24-hour Georgia Model

Finally, canopy temperature was simulated using one equation to represent the diurnal cycle that included other variables such as solar radiation and wind speed (Hake and Silvertooth 1990; Idso et al. 1981) which have been tied to canopy temperature. The 24-hour Georgia Model is provided in Equation 4.5. The model was developed using multiple regression in MATLAB (R2014b) and data collected during the 2013 season.

$$Tc_{24\_hour} = 1.87 + 0.81224 * T_a + 0.8827 * e_a + 0.3188 * U + 0.0010443 * S \quad (4.5)$$

In (4.5), Tc_{24_hour} is the hourly canopy temperature estimated by the model in ˚C, T_a is the mean hourly air temperature in ˚C, e_a is the mean hourly vapor pressure in kPa, U is the mean hourly wind speed in ms^{-1}, and S is the mean hourly solar radiation in Wm^{-2}. This equation was used to calculate modeled values for canopy temperature for Camilla, Georgia during the time periods in 2013 and 2014 in which canopy temperature data were recorded.

Canopy Temperature Forecasts

Canopy temperature forecasts were generated by inputting ECMWF EPS forecast data for the nearest grid point to SIRP into the 24-hour Georgia Model developed above during time periods in 2013 and 2014 in which canopy temperature data were recorded. The ECWMF EPS was used to predict air temperature, vapor pressure, wind speed and solar radiation. The ECMWF EPS consists of a global atmospheric general circulation model, a data assimilation system, a land surface model, an ocean wave model, and an ensemble forecasting system. The horizontal resolution of the model is 0.25˚ (approximately 27 km) (Persson 2011). The model divides the vertical component of the atmosphere into 91 layers covering 64 km at up to 0.1 hPa resolution in the planetary boundary layer, decreasing upward into the stratosphere and lower mesosphere (British Atmospheric Data Centre 2015; Christ et al. 2015a).

In contrast to deterministic forecasts, which provide one model result per grid point, the ECMWF EPS produces multiple model outcomes per grid point that are intended to compensate more adequately for initial analysis and model error. Forecasts such as these are designed to provide a measure of the forecast uncertainty and probability from which alternative scenarios and strategies can be developed. The ECMWF EPS generates a total of 51 forecasts (ensemble members) for each time step,

consisting of the control forecast in addition to 50 perturbed forecasts. These perturbed forecasts are used to represent initial analysis error (by perturbing the initial analysis) and model error (by using stochastic processes to represent errors in model physics). The probability of occurrence of an event (i.e., temperature above or below some threshold) can be characterized by the number of ensemble members predicting the event divided by the total number of members (Christ et al. 2015a; Persson 2011). Using the ECMWF EPS forecasts as inputs to the 24-hr Georgia Model equation provided the generation of ensemble forecasts for canopy temperature during periods in 2013 and 2014 in which canopy temperature measurements were recorded.

Fourier analysis was used to fit the forecast data (issued every 6 hours at 0200, 0800, and 1400 and 2000) to hourly estimates based upon diurnal curves derived from historical data. Historical hourly data for air temperature, dew point and wind speed were provided by the NCDC (http://www.ncdc.noaa.gov) and were recorded at Columbus Metropolitan Airport, Columbus, Georgia, USA from 1980 – 2010. Since the NCDC does not provide hourly solar radiation data, historical hourly data for solar radiation was collected during 2012 at the Camilla, Georgia WeatherNet site provided by the GAEMN (http://www.georgiaweather.net). Dew point temperatures (a measure of atmospheric moisture) were converted to vapor pressure by using Tetens (1930) expression given in Equation 4.6, where e is the vapor pressure in hPa and T_d is the dewpoint temperature in $^{\circ}$C.

$$e = 6.11 * 10^{((7.5*T_d)/(237.3+T_d))} \tag{4.6}$$

Mean Bias Correction

Numerical Weather Prediction (NWP) models frequently display bias with respect to forecasts (Danforth et al. 2007) and statistical techniques can be applied to improve

forecast performance (Christ et al. 2015a; Durai and Bhradwaj 2014; Glahn and Lowry 1972; Hopson and Webster 2010; Shrestha et al. 2014; Webster and Jian 2011). For this study, mean bias corrections were calculated for the 2013 season and applied to the 2014 forecasts. The mean bias for each hour was determined by subtracting the observed canopy temperature from the forecast ensemble mean canopy temperature as shown in Equation 4.7.

$$MB = 1/n \sum_{1}^{n} (EM - obs) \tag{4.7}$$

Where *MB* is the hourly mean bias for a given lead day (10 total) in ˚C, *n* is the number of forecasts included in the season, *EM* is the hourly forecast canopy temperature ensemble mean for a given lead day in ˚C and *obs* is the hourly observed canopy temperature in ˚C. These corrections were applied to the 24-hour forecasts during the 2014 season.

Economic Impact

Probabilistic forecasts can be utilized to determine the cost and risk of applying protective measures to weather-vulnerable assets (Nurmi 2003). For this analysis, risk was defined as the forecast probability of the event multiplied by the estimated loss in yield should heat stress occur as expressed in Equation 4.8.

$$Risk = \Pr_{fcst} * L_{event} \tag{4.8}$$

Where $\Pr_{fcst}$ is the forecast probability and L_{event} is the estimated cost of loss per heat stress event in $\$ha^{-1}$ and defined in Equations 4.9 and 4.10. Equation 4.9 describes

losses occurring in July ($Loss_{July\_event}$) and Equation 4.10 describes those occurring outside July ($Loss_{Aug\_Sep\_event}$).

$$Loss_{July\_event} = Wt_{July} * Yield_{category} / Events_{July} * P_{cotton} \quad (4.9)$$

$$Loss_{Aug\_Sep\_event} = Wt_{Aug\_Sep} * Yield_{category} / Events_{Aug\_Sep} * P_{cotton} \quad (4.10)$$

The L_{event} was estimated using yield losses due to heat stress reported in Brown (2001). The study was conducted over a 13-year period from 1987-1999 in four Arizona counties (Yuma, LaPaz, Maricopa and Pinal). Seasons during the study were ranked in order from the highest to lowest in terms of heat stress accumulated during the primary fruiting cycle. Subsequently, the seasons were classified as low heat stress (four years), intermediate heat stress (five years) and high heat stress (four years). On average, difference in yield between the counties experiencing low heat stress and those experiencing high heat stress was 186 kgha-1 (166 lb/acre), the lowest difference in yield was 112 $kgha^{-1}$ (100 lb/acre) and the highest difference was 285 $kgha^{-1}$ (254 lb/acre). Low, average and high seasonal yield differences were used to divide losses into three categories (conservative loss, intermediate loss and aggressive loss).

Seasonal losses were converted to event losses by assuming the average number of heat stress events occurring within any given year were equal to the number that occurred during 2014, given that 2014 was average, climatologically (NCDC, http://www.ncdc.noaa.gov). The losses were also weighted according to the time of year (Farahani et al. 2012; Oosterhuis and Snider 2011), assuming 75% of the losses occur in July (during reproduction) and 25% of the losses occur in the months after.

Where $Loss_{July\_event}$ and $Loss_{Aug\_Sep\_event}$ are the losses per event in $\$ha^{-1}$ ($/acre) during July and outside July, respectively, and *WtJuly* and Wt_{Aug_Sep} are the weighting applied during July and outside July which were assumed to be 0.75 and 0.25, respectively. $Yield_{category}$ was chosen corresponding to the category of low, intermediate

or high yield losses, assumed to be 112 $kgha^{-1}$ (100 lb/acre), 186 $kgha^{-1}$ (166 lb/acre) and 285 $kgha^{-1}$ (254 lb/acre), respectively. Finally, $Events_{July}$ and $Events_{Aug\_Sep}$ represent the average number of heat stress events assumed to occur within July or outside July, and P_{cotton} is the expected sale price of cotton for the year in consideration in $\$kg^{-1}$ (Shurley and Smith 2013, 2015).

For this analysis, cost was defined as the estimated price of taking action to prevent potential yield losses resulting from a heat stress event. Hake and Silvertooth (1990) suggested that the application of a light irrigation could decrease the impact of heat stress. For this study, a light irrigation was considered to be 0.254cm per event (0.10 in per event). The cost of taking action, $Cost_{event}$, was calculated by multiplying the irrigation applied by the variable cost of irrigation. Variable costs include expenditures for moving the pivot, labor and repairs, as well as maintenance on the motor, pump and pivot, estimated at $\$11.67 ha^{-1} cm^{-1}$ ($12.00/acre-inch) in Shurley and Smith (2013) and $\$9.48/ha^{-1}cm^{-1}$ ($9.75/acre-inch) in Shurley and Smith (2015). The cost equation is provided in Equation 4.11, where *Irrig* was 0.254 cm per event (0.10 inch/event) and the $VarCost_{irrig}$ was $\$11.67\ ha^{-1}cm^{-1}$ ($12.00/acre-inch) in 2013 and $\$9.48\ ha^{-1}cm^{-1}$ ($9.75/acre-inch) in 2015, there was no budget available for 2014. Costs were estimated based upon 2013 and 2015 budgets.

$$Cost_{event} = Irrig * VarCost_{irrig} \tag{4.11}$$

Results

All model results were verified using observed hourly canopy temperature data recorded at SIRP during 2013 and 2014 as mentioned previously in Methods.

Brown and Zeiher Model

R-squared values measuring the fit for the daytime and nighttime models are given in Table 4.2. Values improve substantially from 2013 and 2014. This may be due to the unusually wet growing season of 2013, which led to below normal temperatures in southwest Georgia. By contrast, the 2014 growing season was warmer and drier, which made the environment more similar to conditions in Arizona. Additionally, the Brown and Zeiher Model consistently underestimated canopy temperatures at SIRP during both the daytime and nighttime hours in 2013 and 2014. Theoretically, this may be due to the difference in mean vapor pressures between the Arizona site (where the model was developed) and the Georgia site. The humidity often encountered in the southeastern United States is higher, thus restricting plant cooling and likely resulting in lower modeled canopy temperatures than observed.

Table 4.2. The R^2 values for Canopy Temperature Models Measured during 2013 and 2014. The R^2 value quantifies the nature and strength of a relationship between predictor (canopy temperature model) and predictand (measured canopy temperature). The closer the R^2 value to 1, the better the model fit the observed data.

Year	Model R^2 Value				
	Daytime Brown and Zeiher Model	***Daytime Georgia Model***	***Nighttime Brown and Zeiher Model***	***Nighttime Georgia Model***	***24-hr Georgia Model***
2013	0.73	0.89	0.40	0.87	0.94
2014	0.80	0.88	0.83	0.88	0.93

The Daytime and Nighttime Georgia Models

As discussed above, the Brown and Zeiher Model exhibited a large difference in performance between 2013 and 2014. This difference provided the motivation for developing a model specifically for Georgia. According to data from the National Climatic Data Center (NCDC, http://www.ncdc.noaa.gov), year-to-year variability in temperature and precipitation is common for the region, with some years recording mean temperatures greater than 28°C while others average less than 25°C. A robust canopy temperature model should be able to perform well within this range of observed variability.

The Daytime and Nighttime Georgia Models were developed using data from 2013 and verified using 2014 data. The P-values for the intercept and variable coefficients are listed in Table 4.3 and were less than 0.05, indicating they were statistically significant for both the daytime and nighttime models (referred to as the Daytime Georgia Model and Nighttime Georgia Model, respectively) at a 95% confidence level. Therefore, the intercept and all statistically significant variables were included in the model. The R^2 values are included in Table 4.2 and indicate better fits than the Brown and Zeiher model for both the daytime and nighttime periods during 2013 and 2014. Additionally, there was very little difference in R^2 values between 2013 and 2014 among the Daytime and Nighttime Georgia Models.

Table 4.3. P-values for the Daytime Georgia Model, the Nighttime Georgia Model, and the 24-hour Georgia Model, Developed from Data Recorded in 2013. P-values <0.05 are indicative of model components that have a statistically significant effect upon the model fit at a 95% confidence level. All components listed below were statistically significant.

Models	**P-Values**					
	Intercept	***T_a***	***e_a***	***VPD***	***U***	***S***
Daytime Georgia Model	1.9E -03	3.69E-85	N/A	2.77E-08	N/A	N/A
Nighttime Georgia Model	7.21E -22	3.96E-129	2.09E-03	N/A	N/A	N/A
24-hr Georgia Model	4.35E -05	~ 0	1.36E -08	N/A	1.61E -15	1.08E -11

The 24-hour Georgia Model

The Daytime and Nighttime Georgia Models showed improvement over the results of the Brown and Zeiher Model. Noting it would be more convenient to have a model that represents the complete diurnal cycle, the 24-hour Georgia Model was developed with the addition of two variables (wind and solar radiation) using data from 2013. The P-values for the intercept and equation coefficients are provided in Table 4.3 and were all statistically significant at a 95% confidence interval.

Figure 4.1 shows different plots of the residuals and demonstrate that they resemble a normal distribution, have approximately constant variance, and display no correlation between error size and time, suggesting that the assumptions of linear regression hold thus justifying the use of linear regression to develop the model. The R^2 values are provided in Table 4.2 and indicate a better fit than the previous sets of models for the 2013 and 2014 seasons. There is slight skewing reflected in the histogram and normal probability plot, however, not enough to indicate the residuals are from a different

type of distribution. Further analysis of outliers indicated that the largest residual values were generated when temperature and solar radiation values changed abruptly between hours, most likely indicating a sharp change in cloudiness. Although temperatures were below normal during the 2013 season, the Georgia Model does well fitting the approximately normal and climatologically different 2014 season. The 24-hour Georgia Model was chosen to simulate canopy temperature in this study due to its ease of applicability (one model used for both daytime and nighttime periods) as well as its ability to model canopy temperature well over two climatologically very different years (NCDC, http://www.ncdc.noaa.gov).

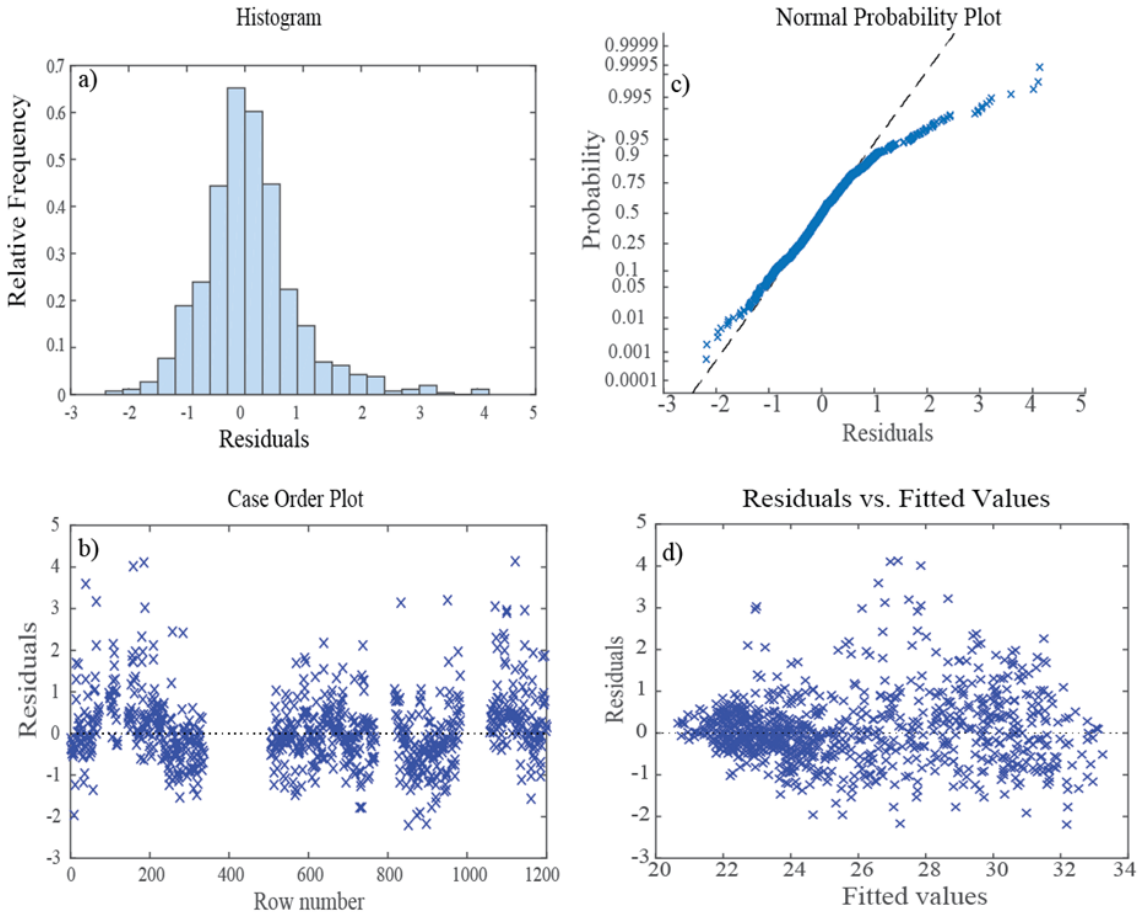

Figure 4.1: a) Histogram, b) Case Order Plot, c) Normal Probability Plot, and d) Residuals vs Fitted Values for the 24-hour Georgia Model. The plots suggest the assumptions of linear regression hold and justify developing the model using linear regression.

Forecast Analysis

This section analyzes and compares the Direct Model Output (DMO) to the bias-corrected canopy temperature forecasts for 2014 alone considering bias corrections were developed from the 2013 forecasts. A popular way to verify and analyze weather forecasts is through the use of contingency tables (Nurmi 2003). Contingency tables separate forecasts into four distinct categories as shown in Table 2.2: hits (a), false alarms

(b), misses (c), and correct rejections (d). The forecasts used in this experiment were converted into simple binary (or yes/no) forecasts using set probability thresholds. Each contingency table had a set probability threshold. Forecasts were grouped into the "yes" category if they exceeded the threshold (Christ et al. 2015a). The highest probability of heat stress occurring during the 24-hour time period was selected as the probability to represent the heat stress forecast for the given day. Contingency tables were created for 2014 from forecast probability thresholds set from 0-100% for the unadjusted DMO as well as for the bias-corrected forecasts.

Relative Operating Characteristic (ROC) diagrams have become a common way to measure forecast performance (Nurmi 2003) as described in Figure 4.2. ROC diagrams were created from the contingency tables developed from the 2014 season by plotting the Hit Rate vs the False Alarm Rate. Equations for the Hit Rate and False Alarm Rate are provided in 4.12 and 4.13, respectively.

$$H = a \big/ (a + c) \tag{4.12}$$

$$F = b \big/ (b + d) \tag{4.13}$$

Where H is the Hit Rate, F is the False Alarm Rate, and a, b, c and d are defined in Table 2.4. The ROC diagrams are presented in Figure 4.2. The diagrams and corresponding ROC areas confirm that both the forecasts for the unadjusted DMO and the bias-corrected forecasts were skillful out to day 10, although the bias-corrected forecasts were more skillful as indicated by higher ROC_a's across all lead days.

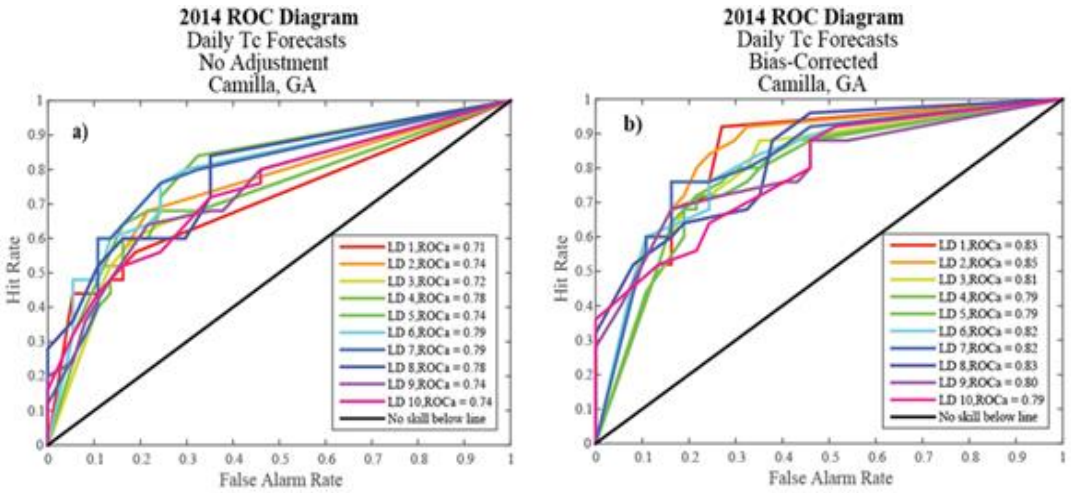

Figure 4.2: a) 2014 Unadjusted Direct Model Output (DMO) and b) 2014 Bias-Corrected Relative Operating Characteristic (ROC) Diagrams. ROC diagrams are plots of the Hit Rate (a measure of the proportion of observed events that were correctly forecast) vs the False Alarm Rate (a measure of the proportion of forecast events that were incorrectly forecast). The closest points to the upper left hand corner of the plot represent the best forecasts. A measure of forecast performance derived from ROC diagrams is the ROC area (ROC_a). It is essentially the area under the curve. In a perfect system, the ROC_a is equal to 1, while a ROC_a less than 0.5 is considered unskillful. In the legend, LD = lead day. ROC_a's are calculated for each forecast lead day.

Besides ROC diagrams, several well-known performance measures can be calculated from contingency tables, among them Correct Warning (CWs) and Missed Events (MEs). CWs occurred when heat stress was observed and the forecast probability was equal to or exceeded a decision threshold. The relationship is provided in Equation 4.14.

$$CW = a/(a+b) \tag{4.14}$$

Where *CW* is the probability that an event will occur given a warning is issued, and variables *a* and *b* are defined in Table 2.4. For example, if a producer decided to

protect against heat stress only when the forecast probability of heat stress exceeded 70%, then a CW occurred when the forecast probability of heat stress was greater than or equal to 70% and heat stress was observed. The higher the probability of CW's at a given threshold, the better the forecast performed with respect to this parameter. Figure 4.3 shows CWs for the unadjusted DMO and bias-corrected 2014 forecasts, respectively. CWs were high for both categories and generally trended upward as forecast probability increased.

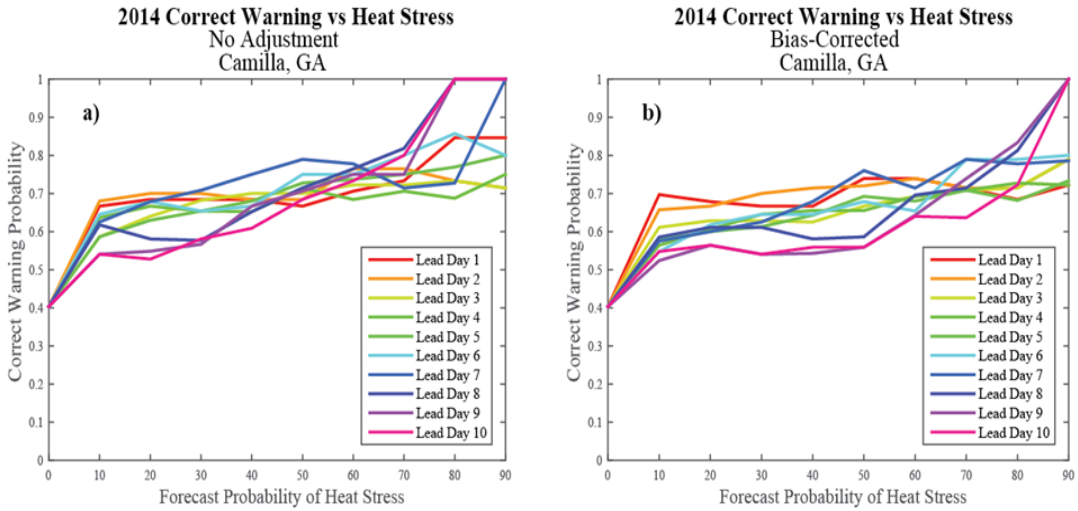

Figure 4.3: a) 2014 Unadjusted Direct Model Output (DMO) and b) 2014 Bias-Corrected Correct Warning (CW) Probability vs Heat Stress. The probability of CW's remained high after applying mean bias corrections to the European Centre for Medium-Range Weather Forecasts (ECMWF) Ensemble Prediction System (EPS) DMO.

MEs occurred when heat stress was observed and the forecast probability was less than a set decision threshold. The relationship is provided in Equation 4.15.

$$ME = c/(a+c) \tag{4.15}$$

Where *ME* is the probability that an event will occur given that no warning is issued. Variables *a* and *c* are defined in Table 2.4. For example, as above, if a producer's decision probability threshold was set at 70%, then a ME occurred when heat stress was observed and the forecast probability was less than 70%. A high rate of MEs would be particularly worrisome for producers who anticipate losses each time heat stress is observed and no action is taken to protect crops. For this application, it is important that forecasts minimize MEs. Figure 4.4 shows MEs for the unadjusted DMO and bias-corrected 2014 forecasts. The number of MEs overall for the bias-corrected category was smaller than unadjusted DMO category, indicating the bias-corrected forecasts were superior.

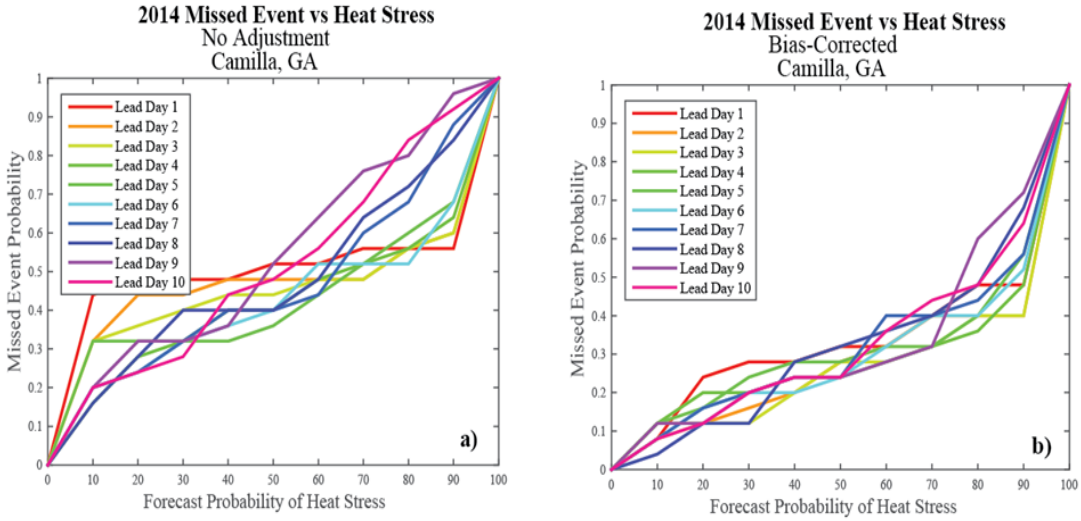

Figure 4.4: a) 2014 Unadjusted and b) 2014 Bias-Corrected Missed Event (ME) Probability vs Heat Stress. The probability of ME's dropped after applying mean bias corrections to the European Centre for Medium-Range Weather Forecasts (ECMWF) Ensemble Prediction System (EPS) Direct Model Output (DMO).

Heat Stress Warning System

Figure 4.5 is an example of heat stress forecasts generated from the probabilistic canopy temperature forecasts developed in this study. These forecasts are designed to warn producers of possible upcoming heat stress events. Figure 4.5.a) represents an 8-day forecast beginning 21 Aug. 2014 (observations were not recorded during the last two days of the period, therefore, reducing the plot to 8 days), and Figure 4.5 b) the 24-hour forecast for 22 Aug. 2014. The 8-day forecast provides daily information concerning medium-term conditions, while the 24-hour forecast presents a more detailed look at each hour during a given day. The 8-day forecast indicates a possible decrease in probability for heat stress late in the period, while the 24-hour forecast appropriately warns when canopy temperatures exceed stress levels within the diurnal cycle.

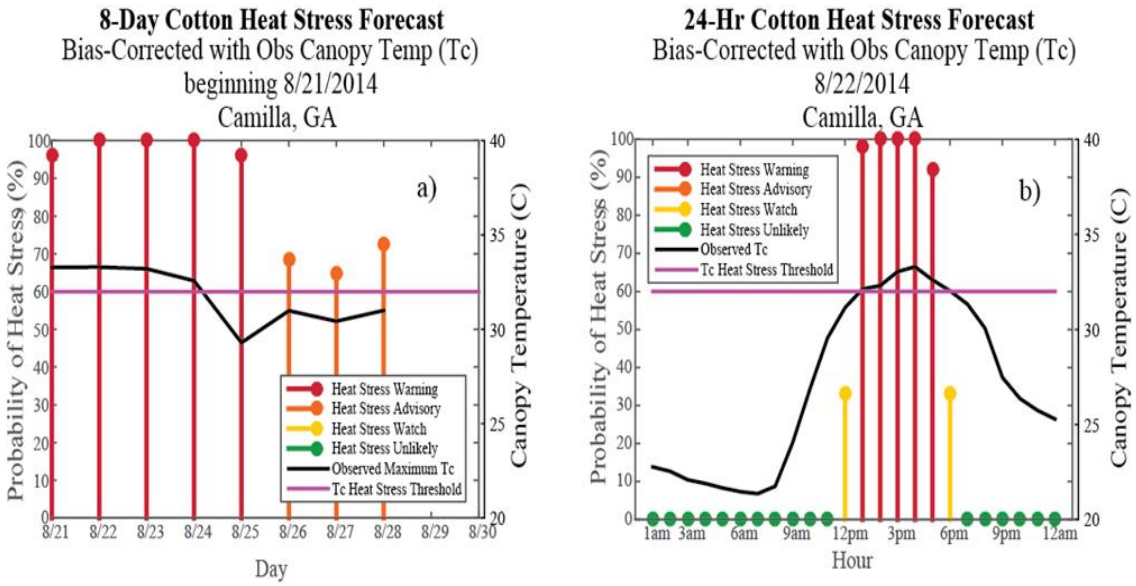

Figure 4.5: a) 8-Day Cotton Heat Stress Forecast beginning 21 Aug. 2014 and b) 24-Hr Cotton Heat Stress Forecast for 22 Aug. 2014 at Camilla, Georgia. Observations for two days at the end of the 10-day period beginning 21 Aug. 2014 were not recorded, therefore, observations and forecasts were not included in the plot. The pink line represents the cotton heat stress threshold defined by the thermal kinetic window (32˚C). Observations above this line indicate heat stress. The black line represents observed canopy temperature. The multi-colored stems represent the heat stress forecast probability (length) and category (color) for the given day (Figure 4.5 a) or hour (Figure 4.5 b). Each stem color represents a probability range of exceeding 32˚C. Red stems indicate a 75% or greater probability, orange stems indicate between a 50% and 75% probability, yellow stems indicate between a 25% and 50% probability, and green stems indicate a 25% or less probability.

Economic Impact

The following is an explanation of how probabilistic forecasts can be utilized to aid producers with financial decisions pertaining to weather-related risks. The analysis provides a way to determine at what forecast probability level a producer should choose to protect based upon risk of loss and cost of protection. Currently, there are few multiple-year studies involving the relationship among canopy temperature, heat stress and yield. Although the study by Brown (2001) was conducted in Arizona and new

cultivars have been developed since its development, the report concentrated on the effects of heat stress related to canopy temperature and yield. Thus, the reason for using it in this illustration.

Risk was calculated for probability levels 0-100% as outlined in Methods, plotted with cost and provided in Figures 4.6 and 4.7. In this illustration, it is evident from Figures 4.6 and 4.7 that the cost to protect in July (during reproduction) is very small compared to the potential losses. Therefore, protecting at very small forecast probabilities works out to be economically responsible. However, the circumstances change somewhat during the August and September timeframes when the cost to protect is closer to risk. Using prices from 2013 (2015) and assuming more conservative losses, one would only protect if the forecast probability were greater than 80% (70%).

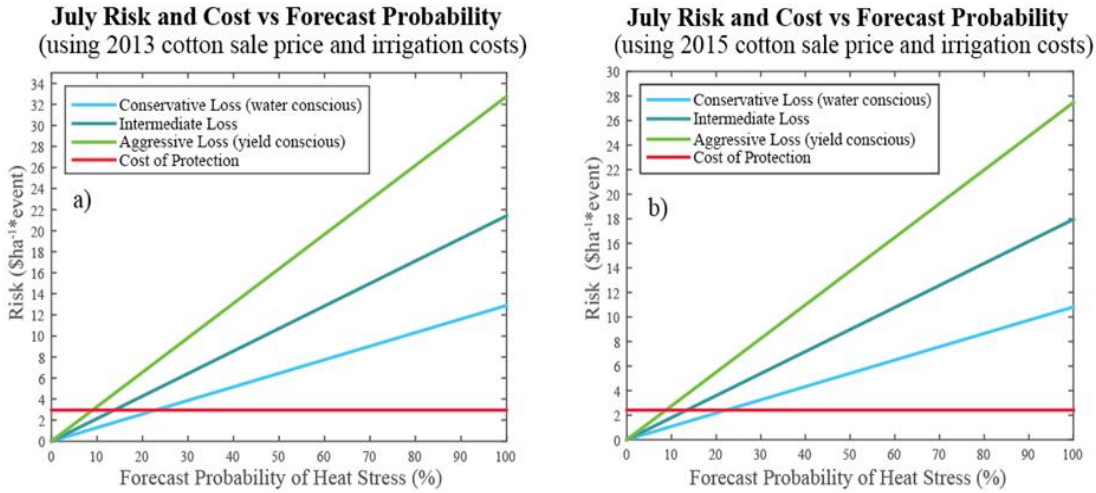

Figure 4.6: a) 2013 and b) 2015 July Risk and Cost vs Forecast Probability. The cost of protection is very low compared to the risk of yield loss during the July time period when plants are most susceptible to heat stress.

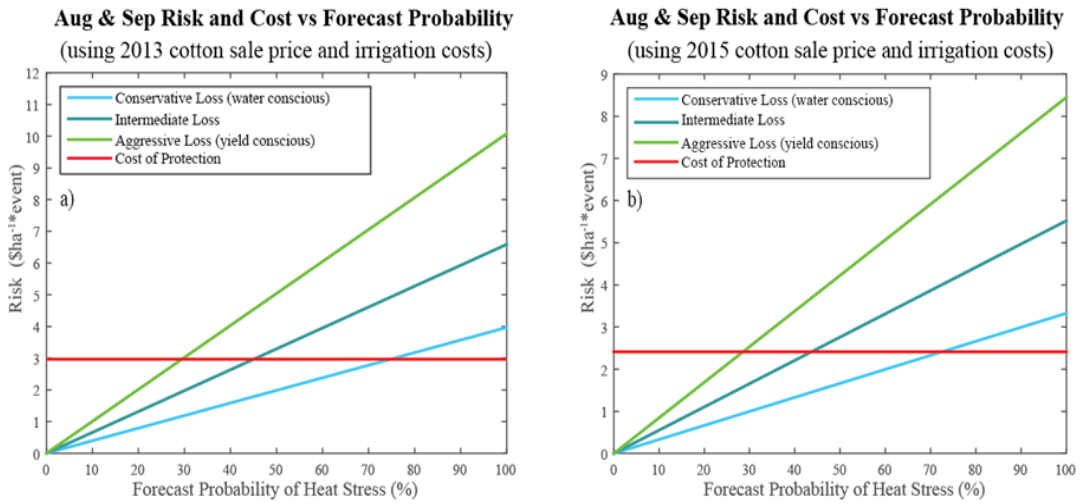

Figure 4.7: a) 2013 and b) 2015 Aug. and Sept. Risk and Cost vs Forecast Probability. Risk decreases later in the season when yield is less likely to be affected by heat stress.

Discussion

The results of this study suggest that it is possible to model canopy temperature based upon air temp, vapor pressure, solar radiation, and wind speed, using a single model for the diurnal period in Georgia. The 24-hr Georgia Model may make it possible to analyze previous years with respect to heat stress and yield. In that sense, it could be used in conjunction with past yield and weather data to better estimate the impact of heat stress on cotton yield. Although the 24-hr Georgia Model fit observations well during the 2013 and 2014 seasons, it would be beneficial to measure its performance further in the coming seasons or using past data. Additionally, it would be advantageous to analyze it with respect to canopy temperature data from other locations in the southeastern United States and worldwide to determine if it can be used over a wider area.

Coupling the 24-hr Georgia Model with the ECMWF EPS created canopy temperature forecasts that were skillful up to 10 days in advance, making it possible to warn producers of upcoming heat stress events. The ECMWF EPS DMO was further

improved using simple statistical mean bias corrections. If forecasts such as these became available to growers, the extended warning period before heat stress events would allow producers time to plan for protecting crops, thus, preventing damage and yield loss. Nonetheless, it would be valuable to measure the performance of the coupled canopy temperature-atmospheric model in multiple locations over multiple growing seasons to determine its skill over a broader range.

The example economic analysis suggests that if variable irrigation costs and cotton sale prices remain within the 2013-2015 price range, it is financially reasonable to protect at very low forecast probabilities during periods in which the plant is most susceptible to heat stress. Beyond those most susceptible periods, expected losses are lower and a producer is free to act more conservatively with respect to protection.

Future Work

In the future, it might be possible to use exogenously applied compounds to protect against heat stress. In that case, the economic analysis performed for this work could be easily adjusted to represent the cost of the spray application. If work is done to quantify the effects of heat stress on yield in the southeastern United States, then this analysis could be updated to include data directly from the region to more accurately estimate the economic impact. The techniques used in this work are adaptable to other regions and other crops. Therefore, similar developments would seem possible for cotton and other crops in different climatic zones.

CHAPTER 5

CONCLUSION

As previously noted, field experiments documented in this work were conducted at SIRP located near Camilla, Georgia. Camilla is situated within a large swath of primarily agricultural land stretching from Alabama to Virginia. The region is characterized by a Humid Subtropical Climate (http://oceanservice.noaa.gov/education/pd/oceans_weather_climate/media/climate_zones.swf), as are several other provinces worldwide including large portions of China, Southeast Asia, India and Brazil. Similarly, these regions are top cotton producers as mentioned in the January 2016 Monthly Economic Letter issued by Cotton, Incorporated (http://www.cottoninc.com/corporate/Market-Data/MonthlyEconomicLetter/). Although important, cotton is not the only crop grown in these regions. Crops such as corn, peanut and soybean are also widely grown in these regions and the strategies developed in this work could be adapted to those as well. Considering the similarities in climate and agricultural land use, the ideas and methodologies developed in this work could be applied globally.

In light of the above, implications for the agricultural community could be significant. Coupled atmospheric-agricultural models have the ability to put weather forecasts in terms producers can understand and can quickly use to make strategic on-farm decisions. Probabilistic forecasts provide growers the additional opportunity to make better decisions based upon more weather information delivered in a concise and easy to understand format. Delivering reliable weather forecasts specifically designed to serve agricultural interests has the potential to make a large positive impact within the industry, and, subsequently, worldwide.

APPENDIX A

PUBLISHED MANUSCRIPT: USING PRECIPITATION FORECASTS TO IRRIGATE COTTON

The *Journal of Cotton Science 19:351–358 (2015)*
http://journal.cotton.org, © The Cotton Foundation 2015

AGRONOMY AND SOILS

Using Precipitation Forecasts to Irrigate Cotton

Emily H. Christ*, Peter J. Webster, Guy D. Collins, Violeta E. Toma, and Seth A. Byrd

ABSTRACT

In this experiment, precipitation forecasts were used to schedule irrigation for cotton (*Gossypium hirsutum* L.). Four irrigation treatments and two cotton varieties were evaluated at Stripling Irrigation Research Park located near Camilla, GA in 2014. Two treatments were irrigated based on forecasts from the European Centre for Medium-Range Weather Forecasts (ECMWF) Ensemble Prediction System (EPS) and The Weather Channel®'s mobile app. Irrigation amounts for these two treatments were determined by the Cotton Irrigation Schedule Suggested for High Yields (check-book recommendations). The third treatment was irrigated by the check-book method and the fourth was rainfed. Irrigation applied for each treatment was 34.8 cm, 26.7cm, and 31.9 cm for the ECMWF EPS, weather.com, and check-book, respectively. Rainfed cotton received 16.56 cm in precipitation. All irrigation methods resulted in significantly higher yields than the rainfed cotton. Results suggest using precipitation forecasts to schedule irrigation could provide a convenient alternative to the check-book method.

Recent droughts throughout the country and the continuing water disputes among the states of Georgia, Alabama, and Florida have made agricultural producers more aware of the importance of managing irrigation systems efficiently. Some southeastern states are beginning to consider laws that will require monitoring and regulation of water used for irrigation. In fact, Georgia recently suspended issuing irrigation permits in some areas to try and limit the amount of water used in irrigation (Hollis, 2013).

Even in southwest Georgia, which receives on average 59.06 cm (23.25 in) of rain during the growing season, irrigation can significantly impact crop yields. Studies have shown there can be large differences between dry-land cotton (*Gossypium hirsutum* L.) production and irrigated yield. For example, Farahani and Munk, 2012 pointed out that if sufficient rainfall fails to occur at critical times during the growth cycle of cotton (during the reproductive stages, from floral budding to peak bloom), yield can be less than half that of irrigated fields.

Many different irrigation scheduling tools are available for producers, some of which include the input of current weather data from nearby stations (Leib et al., 2012). Most published literature concentrating on weather occurring during the growing season emphasizes the role of large-scale patterns on crop production (Baigorria et al., 2008; Hansen et al., 1998, 2001; Paz et al., 2012) and does not investigate the effects of using short-term weather forecasts for management decisions.

Check-book method. In this study, using precipitation forecasts to schedule irrigation is compared to an accepted irrigation practice referred to as the check-book method. The check-book method is a straightforward scheduling aid (University of Georgia Cooperative Extension/ College of Agricultural and Environmental Sciences, 2014). This method has proven to be a simple and effective way to promote high yields.

To follow the method, producers keep a record of observed rainfall and subtract the observed amount from the total amount of irrigation recommended by the Cotton Irrigation Schedule Suggested for High Yields (University of Georgia Cooperative Extension/ College of Agricultural and Environmental Sciences, 2014) provided in Table 1. However, there are caveats to the rule. If an intense, quick rainfall occurs on the field in which runoff is assessed qualitatively by the producer as being high, then the total amount of rainfall in that event may not be subtracted from the recommended amount of irrigation for the time period. Also, if rainfall occurs in the midst of several hot, dry days, then the event would not be subtracted from the recommended amount, if the producer observes the ground to be relatively dry at the time of planned irrigation. During experimentation, the Check-book Treatment was irrigated according to this method.

E.H. Christ*, P.J. Webster, and V.E. Toma, School of Earth and Atmospheric Sciences, Georgia Institute of Technology, 311 Ferst Drive, Atlanta, GA 30332; G.D. Collins, North Carolina State University, Campus Box 7620, Raleigh, NC 27695; and S.A. Byrd, The University of Georgia, PO Box 748, Tifton, GA 31793.
*Corresponding author: echrist3@gatech.edu

Table 1. Cotton Irrigation Schedule Suggested for High Yields and Twice Per Week Application Rates (University of Georgia Cooperative Extension/ College of Agricultural and Environmental Sciences, 2014)

Crop Stage	mm/week	mm/application
Week beginning at 1st bloom	25.4	12.7
2nd week after 1st bloom	38.1	19.0
3rd week after 1st bloom	50.8	25.4
4th week after 1st bloom	50.8	25.4
5th week after 1st bloom	38.1	19.0
6th week after 1st bloom	38.1	19.0
7th week to 1st open boll	25.4	12.7

European Centre for Medium-Range Weather Forecasts (ECMWF) Ensemble Prediction System (EPS) probabilistic precipitation forecasts. The ECMWF EPS generates probabilistic precipitation forecasts. These forecasts were adjusted and used to irrigate the Bias-Adjusted ECMWF EPS Treatment (see Materials and Methods.) The ECMWF EPS consists of a global atmospheric general circulation model, a data assimilation system, a land surface model, an ocean wave model, and an ensemble forecasting system. The horizontal resolution of the model is 0.25° (approximately 27 km) (Persson, 2011). The model divides the vertical component of the atmosphere into 91 layers covering 64 km at up to 0.1 hPa resolution in the planetary boundary layer, decreasing upward into the stratosphere and lower mesosphere (British Atmospheric Data Centre, 2015).

In contrast to deterministic forecasts, which provide one model result per grid point, the ECMWF EPS produces multiple model outcomes per grid point that are intended to compensate more adequately for initial analysis and model error. Forecasts such as these are designed to provide a measure of the forecast uncertainty and probability from which alternative scenarios and strategies can be developed. The ECMWF EPS generates a total of 51 forecasts (ensemble members) for each time step, consisting of the control forecast (the unperturbed model run, which is also run at a finer resolution) in addition to 50 forecasts produced from perturbed model states. These perturbed forecasts are used to represent initial analysis error (by perturbing the initial analysis) and model error (by using stochastic processes to represent errors in model physics). The probability of occurrence of an event (i.e., rainfall above or below some threshold) can be characterized by the number of ensemble members predicting the event divided by the total number of members (Persson, 2011).

Weather.com forecasts. The Weather Channel®'s mobile app (http://www.weather.com/apps) was chosen as the second forecast option due to its accessibility and popularity. Due to its close proximity to Stripling Irrigation Research Park (SIRP), Camilla, GA was set as the forecast location in the app. Unlike the ECMWF EPS, probabilities for precipitation issued by weather.com were not determined based upon a set threshold for an amount of precipitation, but rather upon the probability of receiving any measurable rainfall (considered to be greater than 0.254 mm [0.01 in]).

Although using seasonal weather forecasts for agricultural decision making (e.g., crop and variety decisions) is promising (Crane et al., 2010), the use of more reliable short-term forecasts might have substantial benefits for producers as well. The objective of this experiment was to explore the potential of using precipitation forecasts to schedule irrigation. This is shown by comparing yield, irrigation water use, and forecast performance among the treatments.

MATERIALS AND METHODS

Experimental design. Two cotton varieties, PhytoGen® 499 WRF ('PHY 499 WRF', considered to be more drought tolerant) and FiberMax® 1944 GLB2 ('FM 1944 GLB2', considered to be more responsive to water), were planted in a split block design at the University of Georgia's (UGA) SIRP located near Camilla, GA (31° 16′ 48.288" N, -84° 13′ 10.5594" W, 49 m elevation above sea level). The experiment consisted of four irrigation treatments: Rainfed, Check-book, Weather.com, and Bias-Adjusted ECMWF. Other than differences in irrigation, management practices used throughout the season were consistent across treatments.

Each treatment was replicated three times, with each sub-block consisting of two varieties subjected to one of the four irrigation treatments. Rows were 91 cm (36 in) wide and 13.7 m (45 ft) long. Seeds were sown at 3 seeds/30.5 cm (3 seeds/ft) with a Monosem® (Edwardsville, KS) vacuum planter on 7 May 2014 in Lucy loamy sand, characterized as being very deep, well drained, and moderately permeable. Irrigation was initiated with squaring, which began the week of 8 June 2014 and ceased upon boll opening, which began 30 August 2014. A 3-Span Valley® (Valley, NE) Linear Endfeed 8000 with Nelson® (Walla Walla, WA) S3000 Spinner sprinklers regulated at low pressure was used to ap-

ply irrigation. The drop hose was held constantly at approximately 2.03 m (80 in) from the ground to the base of the sprinkler. A two-row 9930 John Deere® spindle harvester with bagging attachments was used to harvest the crop on 6 October 2014. Seed cotton was ginned through the UGA Microgin.

For the Rainfed Treatment, cotton only received water during the limited number of rainfall events that occurred throughout the 2014 growing season. For the other three treatments, irrigation schedules and amounts were based upon values derived from the Cotton Irrigation Schedule Suggested for High Yields (CISSHY) found in Table 1 (University of Georgia Cooperative Extension/ College of Agricultural and Environmental Sciences, 2014). This table recommends irrigation based upon cotton crop stage and commonly is followed when applying the check-book method of irrigation.

Irrigation was scheduled twice per week on Mondays or Tuesdays for the first application and Thursdays or Fridays for the second, depending upon time and availability at SIRP. Irrigation was applied to all treatments the same day. Irrigation decisions pertaining to the Bias-Adjusted ECMWF Treatment and the Weather.com Treatment were made twice per week on Sunday and Wednesday evenings after observing the forecasts. Irrigation decisions for the Check-book Treatment were made twice per week, the evening before scheduled irrigation. However, if rainfall occurred overnight, adjustments were made the morning of irrigation. During the experiment, 1.27 cm (0.5 in) of water was not applied as prescribed to the two forecast treatments and should be noted as experimental error. The errors occurred during the same irrigation applications for both treatments.

Forecasts are available from the ECMWF EPS twice daily at 0Z and 12Z (8 pm and 8 am EDT). However, many producers are constrained by pivot size and speed to make irrigation decisions only two to three times per week. During this experiment, forecasts using the ECMWF EPS model data were issued twice per week, on Sunday and Wednesday evenings at 1700 (5 pm) EDT and communicated by e-mail. The Sunday evening forecasts included precipitation forecast data from the Sunday 0Z (8 pm EDT Saturday) ECMWF EPS model run, whereas the Wednesday evening forecasts included precipitation forecast data from the Wednesday 0Z (8 pm EDT Tuesday) model run. Forecasts from weather.com were downloaded twice per week on Sunday and Wednesday evenings at 1700 (5 pm) EDT.

Bias adjustments. Numerical Weather Prediction (NWP) models frequently display bias with respect to forecasts (Danforth et al., 2007). In an effort to reduce bias in the ECMWF EPS model forecasts, a statistical technique known as quantile-to-quantile (q-to-q) mapping (Hopson and Webster, 2010, Shrestha et al., 2014, Webster et al., 2011) was applied. For this experiment, q-to-q mapping was performed on each ensemble member to generate a corrected ensemble member forecast. As applied here, the q-to-q technique requires the creation of two cumulative distribution functions (cdfs). One cdf consists of past forecast data the other of past observations for the forecast location (or area) in question. ECMWF model hindcasts (reforecasts for previous years generated once per week using the current version of the model) were used to represent past model forecasts, and observations from the Georgia Automated Environmental Monitoring Network (GAEMN, www.georgiaweather.net) were used to represent past observations. (The process of developing the hindcast and observation cdfs is further explained in the next section.) The q-to-q technique assigns each ensemble member forecast to a quantile on the hindcast cdf. The next step takes the assigned quantile and maps it to a new, "corrected" forecast value on the observation cdf. This bias-correction process is presented in Fig. 1.

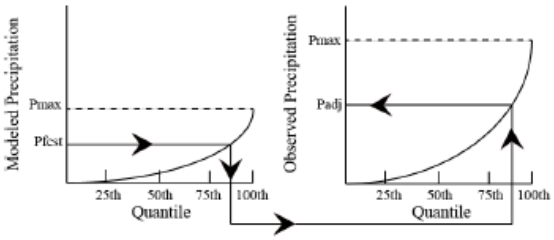

Figure 1. The q-to-q correction system. Both modeled and observed precipitation are binned into quantiles. Precipitation is represented on the y-axis. The modeled precipitation is mapped onto the observed precipitation fields by setting respective modeled quantiles to observed quantiles. In the figure, the forecast precipitation (P_{fcst}) of the 85th quantile is set to the observed precipitation (P_{adj}) of the 85th quantile. (Hopson, et al., 2010)

Hindcasts and observations. In an effort to measure model performance, the ECMWF runs the most current EPS with fewer ensemble members (5 instead of 51) using past data to initialize the run. These are referred to as hindcasts, and they are run for the entire globe once per week for that calendar day over the previous 18 yrs. For this experiment, hindcasts taken from a sampling of grid points near

GAEMN stations in the vicinity of SIRP from 1 May 2013 through 15 August 2013 were used to represent the past model forecasts in a cdf to be used in the q-to-q correction process. For each chosen station, hindcasts from the nearest five grid points were included in the cdf. Cumulative distribution functions were created for each lead day generated by the model. This made it possible to apply q-to-q corrections specifically for every forecast lead day.

Hindcasts from grid points near the following GAEMN stations were included in the model corrections: Camilla (located at SIRP), Tifton, Dawson, Cordele, Newton, Moultrie, Attapulgus and Dixie. The hindcast cdf is represented by the plot on the left-hand side of Fig. 1, with modeled precipitation represented on the y-axis. Observations taken during the time period beginning 1 May and running through mid-August over the previous 18 yrs from the above GAEMN stations were used to generate a cdf of observations. The observation cdf is represented by the plot on the right-hand side of Fig. 1, with observed precipitation represented on the y-axis. Figure 2 shows the hindcasts for lead day one plotted versus the historical observations, illustrating a tendency (bias) to under-predict precipitation for larger observed values. Therefore, the q-to-q corrections helped improve the model's tendency to under-predict precipitation by mapping it to larger values for the same quantile on the observed cdf.

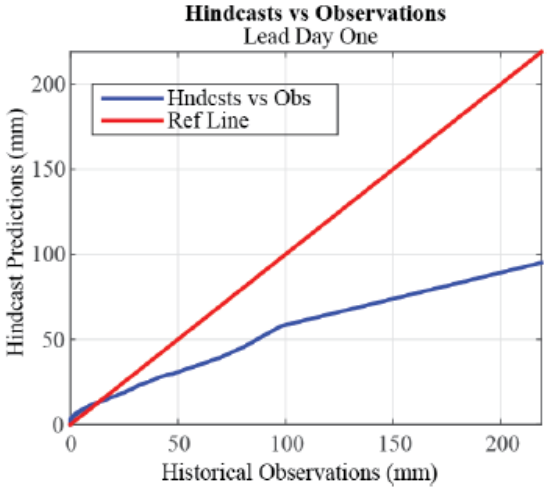

Figure 2. Lead day one plot of hindcasts versus historical observations. Hindcasts tend to over-predict precipitation in the lower values while under-predicting in the upper values.

Bias-adjusted forecasts. The above correction technique was applied to each ensemble member generated by the ECMWF EPS precipitation forecasts, creating 51 Bias-Adjusted ECMWF EPS forecasts for each chosen grid point. Grid points chosen for the forecasts included data from an approximate 1° latitude-longitude box surrounding SIRP. To summarize, there were 51 ensemble members produced at each grid point and 25 grid points chosen for analysis. The forecast probabilities issued were the percent number of ensemble members that predicted at least a threshold value of precipitation would occur as described in Eqs. 1 and 2, below. These Bias-Adjusted ECMWF EPS forecast probabilities were then communicated twice per week via e-mail. An example forecast is shown in Fig. 3.

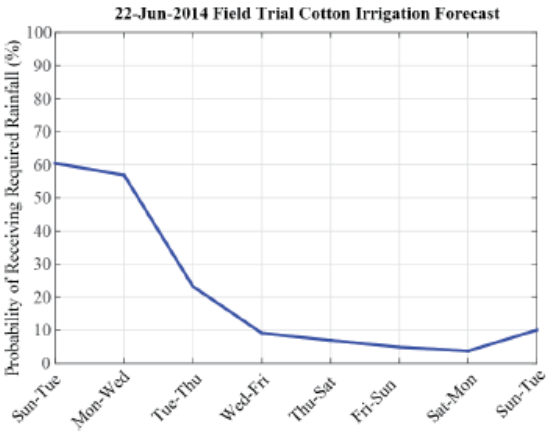

Figure 3. 22 June 2014 Bias-Adjusted ECMWF Treatment forecast.

$$Total\ No\ of\ Ens\ Members = 51\frac{ens\ members}{grid\ point} * 25\ grid\ points = 1275\ Total\ Ens\ Members \quad (1)$$

$$Forecast\ Probability = \frac{number\ of\ ensemble\ members \geq threshold}{total\ number\ of\ ensemble\ members} \quad (2)$$

Precipitation thresholds. Precipitation thresholds were developed for the Bias-Adjusted ECMWF Treatment so that forecast probabilities could be calculated for each time period. Irrigation began upon squaring, and from the onset of irrigation through the first week of bloom, the forecast thresholds were set at 12.7 mm (0.5 in). This threshold matched the CISSHY found in the 2014 UGA Cotton Production Guide provided in Table 1. Following the first week of bloom and for the remainder of season, the forecast thresholds were set at 2.54 mm (0.1 in), 5.08 mm (0.2 in), 7.62 mm (0.3 in), and 10.2 (0.4 in) for each forecast. If the probability of receiving one of the lower precipitation thresholds exceeded the probability limit, then it was subtracted from the total amount recommended by the CISSHY.

Probability limit. A probability limit was set for the experiment so that any forecast exceeding it would trigger cancellation of the planned irrigation. This limit was set somewhat liberally at 60%

to compensate for conservative model estimates of the predominantly convective nature of precipitation occurring in Southwest Georgia during the growing season (Tiedtke, 1989). The decision to irrigate cotton included in the Bias-Adjusted ECMWF Treatment was based upon a 60% probability of exceeding the set threshold amount of precipitation occurring between Monday and Wednesday (for the Sunday-issued forecasts) and Thursday through Sunday (for the Wednesday-issued forecasts). Cotton included in the Bias-Adjusted ECWMF Treatment was irrigated according to the CISSHY, provided in Table 1, when forecast probabilities were less than 60%.

The threshold for irrigation was set at 60% for the weather.com forecasts as well. If there was a 60% chance or more for precipitation during the Monday through Wednesday time period (Sunday forecast) or Thursday through Sunday time period (Wednesday forecast), then irrigation was not applied. Cotton included in the Weather.com Treatment was irrigated according to the CISSHY, provided in Table 1, when forecast probabilities were less than 60%.

Forecast verification. There are many different ways to verify and compare weather forecasts. One common method is by compiling a 2-X-2 contingency table (Nurmi, 2003). Contingency tables separate forecasts into four distinct categories as shown in Table 2: hits (a), false alarms (b), misses (c), and correct rejections (d). Although categorically different, the two forecasts used in this experiment were converted into simple binary (or yes/no) forecasts using a defined probability threshold.

Table 2. 2-X-2 Contingency Table. Contingency tables separate forecasts into four distinct categories (a-d). The variables generated from these categories are used to evaluate forecast performance

Event Forecast	Event Observed		Marginal Total
	Yes	No	
Yes	a[z]	b[y]	(a+b)[x]
No	c[w]	d[v]	(c+d)[u]
Marginal Total	(a+c)[t]	(b+d)[s]	n = (a+b+c+d)[r]

[z] referred to as a Hit.

[y] referred to as a False Alarm.

[x] total number of times the event was forecast.

[w] referred to as a Miss.

[v] referred to as a Correct Rejection.

[u] total number of times the event was not forecast.

[t] total number of times the event was observed.

[s] total number of time the event was not observed.

[r] total number of forecasts in the season.

Binary analysis. Bias-Adjusted ECMWF EPS forecasts were grouped into the "yes" category if the probability of exceeding one of the set threshold precipitation levels exceeded the probability limit (60%); otherwise, the forecasts were grouped into the "no" category. Weather.com forecasts were classified into the yes category if the probability limit was exceeded. Observations were included in the no category for the Bias-Adjusted ECWMF EPS forecasts when the forecasted precipitation threshold was not observed; likewise, forecasts were grouped into the yes category when the threshold was met or exceeded. Similarly for the weather.com forecasts, observations were included in the no category when the recommended amount of precipitation for the time period was not observed and were classified in the yes category when the recommended amount of precipitation for the time period was observed.

Categorical analysis. Several useful variables can be defined based upon combinations and ratios of the different categories contained in a contingency table. These variables are commonly used in the atmospheric sciences to verify and compare forecast performance. In particular, the Hit Rate (HR or Probability of Detection, POD, defined below in Eq. 3) and the False Alarm Ratio (FAR, defined below in Eq. 4) can be used together to evaluate forecast performance. Calculations of HR and FAR for this experiment are included in Table 3 (Nurmi, 2003).

Table 3. Hit Rate, False Alarm Ratio and Bias calculated for the Bias-Adjusted ECMWF EPS and weather.com forecasts. These calculations are used to judge forecast performance

Verification Variable	Bias-Adjusted ECMWF EPS	Weather.com
Hit Rate (HR)	0.2	0
False Alarm Ratio (FAR)	0.6	1
Bias (B)	0.5	1.2

$$HR = a/(a+c) \quad (3)$$

$$FAR = b/(a+b) \quad (4)$$

The HR measures the proportion of observed events that were correctly forecast, whereas the FAR measures the proportion of events incorrectly forecast. Values for HR range between 0 and 1, with 1 being a perfect score, whereas values for FAR vary between 0 and 1, with 0 being a perfect score.

The Bias (B) is also included in Table 3 and defined in Eq. 5. Although Bias is not an indicator of accuracy, it is useful in evaluating how a system

behaves with respect to forecasting a given event (Nurmi, 2003). Bias values greater than 1 indicate the system over-predicts an event, bias values less than 1 indicate the system tends to under-predict, and bias values equal to 1 indicate the system is unbiased.

$$B = (a+b)/(a+c) \quad (5)$$

Statistical analysis. Statistical analysis was performed in MATLAB (R2014b) using two-way analysis of variance (ANOVA) followed by a multiple comparison of means.

RESULTS AND DISCUSSION

The objective of this experiment was to demonstrate the potential of using precipitation forecasts to schedule irrigation. The ECMWF EPS is introduced, with the option to use its forecast data to predict the probability of exceeding predetermined threshold values of precipitation. Bias adjustments and forecast data from the surrounding area are included in the analysis to de-emphasize any sub-grid scale anomalies (such as convective precipitation) occurring at one point that might not be representative of the entire area. It is contrasted with a more common forecast issued by The Weather Channel, which does not provide information pertaining to the amount of rainfall anticipated and is issued for a single location.

Forecast analysis. Table 3 lists the HR and FAR for the Bias-Adjusted ECWMF EPS forecasts and the weather.com forecasts. The Bias-Adjusted ECMWF EPS forecasts out-performed the weather.com forecasts with respect to HR and FAR, although there is room for improvement. It is also interesting to note that the weather.com forecasts did not correctly predict any rainfall events throughout the season, meaning that on the six times the forecast predicted rainfall (13 June, 11 July, 22 July, 25 July, 8 August, and 12 August), none of the events met or exceeded the recommended amount of water for irrigation. Therefore, a producer using these forecasts would have withheld irrigation during time periods in which rainfall either did not occur or the amount of observed was less than the amount recommended.

Q-to-q corrections were applied to the ECMWF EPS forecasts during the experiment in an effort to reduce bias; however, bias remained. Values for B found in Table 3 indicate that the Bias-Adjusted ECMWF EPS system tended to under-predict rainfall events, whereas the weather.com forecasts tended to over-predict precipitation. From a producer standpoint, it could be more beneficial to choose a forecast system that, to an extent, tends to under-predict rainfall rather than over-predict, thus protecting against water stress. If this were the case, the Bias-Adjusted ECMWF EPS forecasts would be a better choice both in terms of B and overall forecast performance.

Water applied. Total water applied for each treatment was calculated by summing all the irrigation applications during the season. Water applied over the course of the season totaled 34.80 cm, 31.93 cm, and 26.67cm for the Bias-Adjusted ECMWF, the Weather.com, and Check-book treatments, respectively. The larger amount of water applied to the Bias-Adjusted ECMWF Treatment reflects the tendency to under-predict rainfall indicated by the values for B calculated in the previous section. Similarly, the smaller amount of water applied to the Weather.com Treatment reflects the tendency for these forecasts to over-predict precipitation.

Yield. Yields from the Bias-Adjusted ECMWF Treatment were the greatest followed by the Weather.com Treatment, the Check-book Treatment, and the Rainfed Treatment, averaging 1796 kg/ha, 1717 kg/ha, 1692 kg/ha and 730 kg/ha, respectively. Because there was no interaction between irrigation method and cultivar, the statistical analyses for the two varieties were combined and are presented in Table 4. The results show that yields from the Rainfed Treatment are significantly different (lower) than the irrigated treatments. There is no significant difference among yields of the irrigated treatments (the Check-book Treatment, the Bias-Adjusted ECWMF Treatment, or the Weather.com Treatment) at a 95% confidence level.

Table 4. Statistical Analysis. Two-way analysis of variance (ANOVA) followed by a multiple comparison of means was performed as the statistical analysis. Because there was no interaction between irrigation method and cultivar, the statistical analyses for the two varieties were combined

Yield Comparison between Treatments		*p*-values[z]
Check-book Trtmt	Bias-Adjusted Trtmt	4.00E-01
Check-book Trtmt	Weather.com Trtmt	1.00
Check-book Trtmt	Rainfed Trtmt	0.00
Bias-Adjusted ECMWF Trtmt	Weather.com Trtmt	6.0E-01
Bias-Adjusted ECMWF Trtmt	Rainfed Trtmt	0.00
Weather.com Trtmt	Rainfed Trtmt	0.00

[z] *p*-values < 0.05 indicate statistically significant differences in mean yields.

The Check-book Treatment was included primarily as a yield comparison for the two forecast treatments. The results of this short study indicate that it might be possible to use precipitation forecasts to maintain yield at levels comparable to those one would expect using the check-book method. Therefore, instead of keeping record of past rainfall as with the check-book method, producers could save time by simply looking at the precipitation forecast to schedule irrigation.

FUTURE WORK

The creation of a forecast system designed to serve agricultural interests and provide information specifically tailored for the agricultural industry has the potential to make a large positive impact both within and beyond the irrigation sector. To accomplish this, however, work needs to be done to improve the accuracy of ECMWF EPS and weather.com forecasts in southern Georgia and other areas of intense agricultural industry. Work has begun to characterize the ECMWF EPS performance over the southern Georgia region. This work will be key in determining how to improve forecast accuracy. Once the forecasts have been optimized, it would be beneficial to run a series of field trials over a period of several seasons to further study the usefulness of precipitation forecasts with respect to scheduling irrigation.

Additionally, more research needs to be done on the manner and timing in which forecasts are used. There are many different methods producers use to irrigate. The only one explored in this research was the check-book method. Therefore, it would be constructive to use precipitation forecasts in conjunction with additional methods such as the use of sensor systems to see if results could be further optimized.

ACKNOWLEDGMENTS

This research has been supported by Cotton, Inc. We are indebted to ECMWF for providing data to make this analysis possible. We wish to thank Kater Hake and Ed Barnes for comments on the project.

REFERENCES

Baigorria, G.A., J.W. Hansen, N. Ward, J.W. Jones, and J.J. O'Brien. 2008. Assessing predictability of cotton yields in the southeastern United States based on regional atmospheric circulation and surface temperatures. J. Appl. Meteorol. 47:76–91. doi:10.1175/2007jamc1523.1.

British Atmospheric Data Centre. 2015. European Centre for Medium-Range Weather Forecasts atmospheric level types [Online]. Available at http://badc.nerc.ac.uk/data/ecmwf-op/levels.html (verified 24 Sep. 2015).

Crane, T.A., C. Roncoli, J. Paz, N. Breuer, K. Broad, K.T. Ingram, and G. Hoogenboom. 2010. Forecast skill and farmers' skills: Seasonal climate forecasts and agricultural risk management in the southeastern United States. Weather Clim. Soc. 2:44–59. doi:10.1175/2010wcas1075.1.

Danforth, C.M., E. Kalnay, and T. Miyoshi. 2007. Estimating and correcting global weather model error. Mo. Weather Rev. 135: 281–299. doi:10.1175/mwr3289.1.

Farahani, H., and D. Munk. 2012. Why irrigate cotton? p. 2–6 *In* C. Perry and E. Barnes (ed.), Cotton Irrigation Management for Humid Regions. Cotton Incorporated, Cary, NC.

Hansen, J.W., A.W. Hodges, and J.W. Jones. 1998. ENSO influences on agriculture in the southeastern United States. J. Clim. 11:404–411. doi:10.1175/1520-0442(1998)011<0404:eioait>2.0.co;2.

Hansen, J.W., J.W. Jones, A. Irmak, and F. Royce. 2001. El Nino-Southern Oscillation impacts on crop production in the southeast United States. p. 57–78 *In* J.L. Hatfield et al. (eds.), Impacts of El Nino and Climate Variability on Agriculture. American Society of Agronomy, Madison, WI.

Hollis, P. 2013. Irrigation scheduling tools seen as a key to conserving water in southwest Georgia. Southeast Farm Press [Online]. Available at http://southeastfarmpress.com/equipment/irrigation-scheduling-tools-seen-key-conserving-water-southwest-georgia (verified 17 Sep. 2015).

Hopson, T.M., and P.J. Webster. 2010. A 1-10-day ensemble forecasting scheme for the major river basins of Bangladesh: forecasting severe floods of 2003-07. J. Hydrometeorology 11:618–641. doi:10.1175/2009jhm1006.1.

Leib, B., G. Sassenrath, and A.M. Schmidt. 2012. Irrigation scheduling tools. p. 32–37 *In* C. Perry and E. Barnes (eds.), Cotton Irrigation Management for Humid Regions. Cotton Incorporated, Cary, NC..

Nurmi, P. 2003. Recommendations on the verification of local weather forecasts (at ECMWF Member States). Series: ECMWF Technical Memoranda. European Centre for Medium-Range Weather Forecasts, Reading, England.

Paz, J.O., P. Woli, A. Garcia y Garcia, and G. Hoogenboom. 2012. Cotton yields as influenced by ENSO at different planting dates and spatial aggregation levels. Agric. Syst. 111:45–52. doi:10.1016/j.agsy.2012.05.004.

Persson, A. 2011. User guide to ECMWF forecast products. European Centre for Medium-Range Weather Forecast, Reading, UK.

Shrestha, K.Y., P.J. Webster, and V.E. Toma. 2014. An atmospheric-hydrologic forecasting scheme for the Indus River basin. J. Hydrometeorology 15:861–890. doi:10.1175/jhm-d-13-051.1.

Tiedtke, M. 1989. A comprehensive mass flux scheme for cumulus parameterization in large-scale models. Mo. Weather Rev. 117:1779–1800. doi:10.1175/1520-0493(1989)117<1779:acmfsf>2.0.co;2.

University of Georgia Cooperative Extension/College of Agricultural and Environmental Sciences. 2014. 2014 Georgia cotton production guide. Cooperative Extension Service/University of Georgia, Tifton, GA.

Webster, P.J., V.E. Toma, and H.M. Kim. 2011. Were the 2010 Pakistan floods predictable? Geophys. Res. Lett. 38:L04806. doi:10.1029/2010gl046346.

APPENDIX B

SUBMITTED MANUSCRIPT: PREDICTING HEAT STRESS IN COTTON USING PROBABILISTIC CANOPY TEMPERATURE FORECASTS

TITLE: Predicting Heat Stress in Cotton Using Probabilistic Canopy Temperature Forecasts

AUTHORS:

Emily H. Christ (corresponding author)
School of Earth and Atmospheric Sciences
Georgia Institute of Technology
311 Ferst Drive
Atlanta, GA 30332
Phone: 256-431-7077
E-mail: echrist3@gatech.edu

Peter J. Webster
(Same as Emily Christ)

John L. Snider
Crop & Soil Sciences
The University of Georgia
115 Coastal Way
Tifton, GA 31794

Violeta E. Toma
(Same as Emily Christ)

Derrick M. Oosterhuis
Dale Bumpers College of Agricultural, Food and Life Sciences
The University of Arkansas
1366 Altheimer Dr.
Fayetteville, AR 72704-6804

Daryl R. Chastain
Delta Research and Extension Center
Mississippi State University
PO Box 197
Stoneville, MS 38776

ABSTRACT

As in humans, heat stress can cause many adverse effects to exposed crops by reducing yield or causing total crop failure. This study was conducted to determine if it is possible to predict heat stress in the Camilla, Georgia region out to 10-days for cotton (*Gossypium hirsutum* L.), providing time for growers to use protective measures. We define plant heat stress as those time periods during which the canopy temperature exceeds the upper limit on the Thermal Kinetic Window (TKW). Noting that a cotton canopy temperature model developed for Arizona yielded relatively poor results for the Camilla region, a new model was developed using a linear regression approach. Model results were evaluated using observed canopy temperature data recorded at Stripling Irrigation Research Park (SIRP). The canopy temperature model was coupled with an atmospheric model, the European Centre for Medium-Range Weather Forecasts (ECMWF) Ensemble Prediction System (EPS), and 10-day probabilistic canopy temperature forecasts were generated for each day of observations during 2014. Subsequently, a statistical mean bias correction was applied to improve upon the Direct Model Output (DMO). Medium term forecasts (10-day) as well as 24-hour forecasts were developed as part of a heat stress warning system. Predictive skill was found out to 10 days, and the bias-corrected forecasts were more skillful than the DMO. Additionally, an economic analysis was performed as an example of how probabilistic forecasts can be utilized to aid producers with financial decisions pertaining to weather-related risks.

Abbreviations: AZMET, Arizona Meteorological Network; CW, Correct Warning; DMO, Direct Model Output; ECMWF, European Centre for Medium-Range Weather Forecasts; EPS, Ensemble Prediction System; GAEMN, Georgia Automated Environmental Modeling Network;

ME, Missed Event; NCDC, National Climatic Data Center; ROC, Relative Operating Characteristic; SIRP, Stripling Irrigation Research Park; TKW, Thermal Kinetic Window

INTRODUCTION

The effects of high temperature stress on humans have been well documented. Prolonged exposure to elevated temperatures can cause heat stroke, heat exhaustion, heat cramps, premature births, and a range of health risks (Centers for Disease Control and Prevention 2014). These conditions are caused when the body's normal cooling mechanisms of vasodilation and perspiration are overcome, allowing the core body temperature to rise to unhealthy levels. At very high body temperatures, permanent damage can occur to the brain and other vital organs and can even lead to death (Centers for Disease Control and Prevention 2006). The heat wave that engulfed France during a 20 day period in August 2003 made worldwide headlines by claiming over 14,000 lives, and similar scenarios have played out all over the world (Kovats and Hajat 2008). Already this year in May, India experienced a heat wave that took the lives of over 1,000 people (Bhalla 2015). Fortunately, one city in India had put a plan in place to prepare for extreme heat. Ahmedabad's "Heat-Health Action Plan" (Knowlton et al. 2014) uses 7-day probabilistic weather forecasts to forewarn city leaders concerning impending heat waves. These forecasts allowed time to implement mitigatory resources for those in society threatened by heat.

Although somewhat less in the public mind, high temperature stress occurs in plants as well. Plants, similar to humans, have cooling mechanisms for temperature regulation during times of extreme heat. In cotton (*Gossypium hirsutum* L.), cooling is accomplished by opening stomates in the leaves, allowing evaporation to cool the plant when it becomes too warm. This

mechanism works quite well, especially in dry climates where evaporative cooling can be very effective. For example, in Arizona, with air temperatures measuring 49˚C, well-watered cotton plant canopy temperatures were measured at 31˚C compared to canopy temperatures in water stressed fields that reached 40˚C (Hake and Silvertooth 1990). Therefore, as with humans, the natural cooling mechanism in plants can be overcome under certain conditions, causing irreversible damage and even death to the plant.

The effects of high temperature stress on cotton were reviewed in Oosterhuis and Snider (2011). Among these effects are decreased growth rate, decreased photosynthesis, and decreased membrane integrity. High night temperatures have been shown to increase respiration rates, decrease soluble carbohydrate concentrations in source leaves, and increase boll abscission or shedding. Because reproductive development is particularly sensitive to high temperature stress, it has also been linked to lower yield. More specifically, decreased yield due to high temperatures has been tied to fewer bolls per plant and smaller boll size (Snider and Oosterhuis 2015). Reddy el al. (1992) attributes decreased boll mass to higher rates of boll abscission in accord with subsequent studies (Lokhande and Reddy, 2014; Reddy et al., 1999; Zhao et al., 2005). Pettigrew (2008) associates smaller boll size caused by high temperatures to a decreased number of seeds per boll, which likely limits fertilization efficiency (reviewed in Oosterhuis and Snider, 2011; Snider and Oosterhuis, 2011, 2012).

Defining Heat Stress

Mahan and Upchurch (1988) and Upchurch and Mahan (1988) suggest that plants have the ability to maintain a normative temperature. Plants have the ability to do this in a limited manner such that environmental temperatures less than the optimum (for cotton, 27 ± 2°C) are set by the environment. These studies suggest three constraints on maintenance of the normative temperature: (1) sufficient energy influx to raise plant temperature to the normative value, (2) a sufficient water supply for transpiration, and (3) humidity levels low enough to allow for evaporative cooling. During periods when ambient temperatures exceed the optimum value, plants abiding the three constraints can maintain canopy temperatures less than the environment and within 2°C of the ideal. This maintenance was accomplished by transpirational cooling.

Transpiration effects also can be present at night. For example, Upchurch and Mahan (1988) reported plant temperatures within 2°C of the normative temperature while the environmental temperatures were found to be as high as 39°C during the nighttime hours. This suggests that plants are able to regulate a constant ideal temperature for the plant throughout the diurnal cycle.

The normative temperature has been tied to the Thermal Kinetic Window (TKW) for enzyme activity. The TKW has been defined as the range of plant temperatures at which the Michaelis constant, Km, of an important metabolic enzyme is at or below 200% of the minimum observed value (Mahan et al. 1990). Due to its link to efficient enzyme function, the TKW correlates strongly with optimal temperatures for general metabolism and growth for various species (Burke et al. 1988, Burke 1990). The TKW for cotton has been determined to be

between 23.5 and 32˚C (Burke et al. 1988). We define time periods of heat stress to include hours during the diurnal cycle in which the canopy temperature exceeds the upper limit of the TKW.

Rationale

Creating advisories for cotton that are similar to those used to warn humans of impending periods of heat stress has the advantage of informing producers of damaging conditions ahead of time. The ability to predict heat stress several days in advance would provide growers the opportunity to put protective measures in place before damage is done. In this work, a cotton canopy temperature model is developed and coupled with an atmospheric predictive model, producing canopy temperature forecasts out to 10 days. Subsequently, a heat stress warning system is developed and analyzed. The warning system is designed to provide information pertaining to the probability of heat stress occurring during the forecast period. Additionally, a short economic analysis is included that estimates the cost to protect against heat stress based upon forecast probability and the possible losses incurred. The economic analysis is intended to be viewed as an example of how probabilistic forecasts can be used to help growers make financial decisions pertaining to weather-related risks.

METHODS

Mean hourly average canopy temperatures were recorded for well-watered cotton plants during 2013 and 2014 at the University of Georgia's (UGA's) Stripling Irrigation Research Park (SIRP) located near Camilla, Georgia (31˚ 16' 48.288" N, -84˚ 13' 10.5594" W, 49 m elevation above sea level). Canopy temperature measurements were recorded from 5 July 2013 through 23 August 2013 and 7 July 2014 through 1 October 2014 using SmartCrop® infrared sensors.

Sensors were arranged and measured according to Snider et al. (2015). Dates that were excluded from analysis during the 2013 and 2014 seasons during which sensors were inoperative or pesticides were being applied are provided in Table 1. Data from the Georgia Automated Environmental Monitoring Network (GAEMN, www.georgiaweather.net) collected at the Camilla, Georgia field site were used to model real-time hourly canopy temperature. The following three sections describe the methods used to analyze and develop several canopy temperature models.

Brown and Zeiher Model

Brown and Zeiher (1998) developed cotton canopy temperature models that accounted for ambient air temperature, vapor pressure and vapor pressure deficit. The models were developed based upon observations obtained from the AZMET (The Arizona Meteorological Network, http://ag.arizona.edu/azmet) and field measurements of canopy temperature. One model was used to predict daytime canopy temperatures, while a second version was used to predict nighttime canopy temperatures as expressed in equations (1) and (2) below:

$$Tc_{daytime} = 0.53 + T_a - 1.43 * VPD \quad (1)$$

$$Tc_{nighttime} = -5.93 + T_a + 1.95 * e_a \quad (2)$$

Here, T_c is the hourly canopy temperature estimated by the model in ˚C, T_a is the measured mean hourly ambient environmental air temperature in ˚C, VPD is the mean hourly measured vapor pressure deficit in kPa, and e_a is the mean hourly vapor pressure in kPa. The daytime equation was used for time periods after sunrise and before sunset, while the nighttime equation was used between sunrise and sunset (United States Naval Observatory Astronomical

Applications Department, http://aa.usno.navy.mil). These equations were used to calculate modeled values for canopy temperature for Camilla, Georgia during the time periods in 2013 and 2014 in which canopy temperature data were recorded.

The Daytime and Nighttime Georgia Models

Daytime and nighttime canopy temperatures were simulated during the 2014 season using the same variables as in the Brown and Zeiher (1998) model (air temperature and vapor pressure deficit (day) and air temperature and vapor pressure (night)). The models were developed using multiple regression in MATLAB (R2014b) and data collected during the 2013 season. They are provided in equations 3 and 4.

$$Tc_{daytime,GA} = -3.5529 + 1.1728 * T_a - 1.2001 * VPD \quad (3)$$

$$Tc_{nighttime,GA} = 4.2153 + 0.74375 * T_a + 0.67888 * e_a \quad (4)$$

These equations were used to calculate modeled values for canopy temperature for Camilla, Georgia during the time periods in 2013 and 2014 in which canopy temperature data were recorded.

The 24-hour Georgia Model

Finally, canopy temperature was simulated using one equation to represent the diurnal cycle that included other variables such as solar radiation and wind speed (Idso et al. 1981, Hake and Silvertooth 1990) which have been tied to canopy temperature. The 24-hour Georgia Model

is provided in equation 5. The model was developed using multiple regression in MATLAB (R2014b) and data collected during the 2013 season.

$$Tc_{24\_hour} = 1.87 + 0.81224 * T_a + 0.8827 * e_a + 0.3188 * U + 0.0010443 * S \quad (5)$$

In (5), Tc_{24_hour} is the hourly canopy temperature estimated by the model in ˚C, T_a is the mean hourly air temperature in ˚C, e_a is the mean hourly vapor pressure in kPa, U is the mean hourly wind speed in ms^{-1}, and S is the mean hourly solar radiation in Wm^{-2}. This equation was used to calculate modeled values for canopy temperature for Camilla, Georgia during the time periods in 2013 and 2014 in which canopy temperature data were recorded.

Canopy Temperature Forecasts

Canopy temperature forecasts were generated by inputting ECMWF EPS forecast data for the nearest grid point to SIRP into the 24-hour Georgia Model developed above during time periods in 2013 and 2014 in which canopy temperature data were recorded. The ECWMF EPS was used to predict air temperature, vapor pressure, wind speed and solar radiation. The ECMWF EPS consists of a global atmospheric general circulation model, a data assimilation system, a land surface model, an ocean wave model, and an ensemble forecasting system. The horizontal resolution of the model is 0.25˚ (approximately 27 km) (Persson 2011). The model divides the vertical component of the atmosphere into 91 layers covering 64 km at up to 0.1 hPa resolution in the planetary boundary layer, decreasing upward into the stratosphere and lower mesosphere (British Atmospheric Data Centre 2015, Christ et al. 2015).

In contrast to deterministic forecasts, which provide one model result per grid point, the ECMWF EPS produces multiple model outcomes per grid point that are intended to compensate more adequately for initial analysis and model error. Forecasts such as these are designed to provide a measure of the forecast uncertainty and probability from which alternative scenarios and strategies can be developed. The ECMWF EPS generates a total of 51 forecasts (ensemble members) for each time step, consisting of the control forecast in addition to 50 perturbed forecasts. These perturbed forecasts are used to represent initial analysis error (by perturbing the initial analysis) and model error (by using stochastic processes to represent errors in model physics). The probability of occurrence of an event (i.e., temperature above or below some threshold) can be characterized by the number of ensemble members predicting the event divided by the total number of members (Persson 2011, Christ et al. 2015). Using the ECMWF EPS forecasts as inputs to the 24-hr Georgia Model equation provided the generation of ensemble forecasts for canopy temperature during periods in 2013 and 2014 in which canopy temperature measurements were recorded.

Fourier analysis was used to fit the forecast data (issued every 6 hours at 0200, 0800, and 1400 and 2000) to hourly estimates based upon diurnal curves derived from historical data. Historical hourly data for air temperature, dew point and wind speed were provided by the NCDC (http://www.ncdc.noaa.gov) and were recorded at Columbus Metropolitan Airport, Columbus, Georgia, USA from 1980 – 2010. Since the NCDC does not provide hourly solar radiation data, historical hourly data for solar radiation was collected during 2012 at the Camilla, Georgia WeatherNet site provided by the GAEMN (http://www.georgiaweather.net). Dew point temperatures (a measure of atmospheric moisture) were converted to vapor pressure by using

Tetens (1930) expression given in equation 6, where e is the vapor pressure in hPa and T_d is the dewpoint temperature in ˚C.

$$e = 6.11 * 10^{((7.5*T_d)/(237.3+T_d))} \quad (6)$$

Mean Bias Correction

Numerical Weather Prediction (NWP) models frequently display bias with respect to forecasts (Danforth et al. 2007) and statistical techniques can be applied to improve forecast performance (Glahn and Lowry 1972, Hopson and Webster 2010, Webster and Jian 2011, Durai and Bhradwaj 2014, Shrestha et al. 2014, Christ et al. 2015). For this study, mean bias corrections were calculated for the 2013 season and applied to the 2014 forecasts. The mean bias for each hour was determined by subtracting the observed canopy temperature from the forecast ensemble mean canopy temperature as shown in equation 7.

$$MB = \frac{1}{n}\sum_{1}^{n}(EM - obs) \quad (7)$$

Where MB is the hourly mean bias for a given lead day (10 total) in ˚C, n is the number of forecasts included in the season, EM is the hourly forecast canopy temperature ensemble mean for a given lead day in ˚C and obs is the hourly observed canopy temperature in ˚C. These corrections were applied to the 24-hour forecasts during the 2014 season.

Economic Impact

Probabilistic forecasts can be utilized to determine the cost and risk of applying protective measures to weather-vulnerable assets (Nurmi 2003). For this analysis, risk was defined as the forecast probability of the event multiplied by the estimated loss in yield should heat stress occur as expressed in Equation 7.

$$Risk = P_{fcst} * L_{event} \quad (7)$$

Where P_{fcst} is the forecast probability and L_{event} is the estimated cost of loss per heat stress event in \$ha^{-1} and defined in equations 8 and 9. Equation 8 describes losses occurring in July ($Loss_{July\_event}$) and equation 9 describes those occurring outside July ($Loss_{Aug\_Sep\_event}$).

$$Loss_{July\_event} = Wt_{July} * Yield_{category} / Events_{July} * P_{cotton} \quad (8)$$

$$Loss_{Aug\_Sep\_event} = Wt_{Aug\_Sep} * Yield_{category} / Events_{Aug\_Sep} * P_{cotton} \quad (9)$$

The L_{event} was estimated using yield losses due to heat stress reported in Brown (2001). The study was conducted over a 13-year period from 1987-1999 in four Arizona counties (Yuma, LaPaz, Maricopa and Pinal). Seasons during the study were ranked in order from the highest to lowest in terms of heat stress accumulated during the primary fruiting cycle. Subsequently, the seasons were classified as low heat stress (four years), intermediate heat stress (five years) and high heat stress (four years). On average, difference in yield between the counties experiencing low heat stress and those experiencing high heat stress was 186 kgha-1 (166 lb/acre), the lowest difference in yield was 112 kgha^{-1} (100 lb/acre) and the highest

difference was 285 $kgha^{-1}$ (254 lb/acre). Low, average and high seasonal yield differences were used to divide losses into three categories (conservative loss, intermediate loss and aggressive loss).

Seasonal losses were converted to event losses by assuming the average number of heat stress events occurring within any given year were equal to the number that occurred during 2014, given that 2014 was average, climatologically (NCDC, http://www.ncdc.noaa.gov). The losses were also weighted according to the time of year (Oosterhuis and Snider 2011, Farahani et al. 2012), assuming 75% of the losses occur in July (during reproduction) and 25% of the losses occur in the months after.

Where $Loss_{July\_event}$ and $Loss_{Aug\_Sep\_event}$ are the losses per event in $\$ha^{-1}$ ($/acre) during July and outside July, respectively, and Wt_{July} and Wt_{Aug_Sep} are the weighting applied during July and outside July which were assumed to be 0.75 and 0.25, respectively. $Yield_{category}$ was chosen corresponding to the category of low, intermediate or high yield losses, assumed to be 112 $kgha^{-1}$ (100 lb/acre), 186 $kgha^{-1}$ (166 lb/acre) and 285 $kgha^{-1}$ (254 lb/acre), respectively. Finally, $Events_{July}$ and $Events_{Aug\_Sep}$ represent the average number of heat stress events assumed to occur within July or outside July, and P_{cotton} is the expected sale price of cotton for the year in consideration in $\$kg^{-1}$ (Shurley and Smith 2013, Shurley and Smith 2015).

For this analysis, cost was defined as the estimated price of taking action to prevent potential yield losses resulting from a heat stress event. Hake and Silvertooth (1990) suggested that the application of a light irrigation could decrease the impact of heat stress. For this study, a

light irrigation was considered to be 0.254cm per event (0.10 in per event). The cost of taking action was calculated by multiplying the irrigation applied by the variable cost of irrigation. Variable costs include expenditures for moving the pivot, labor and repairs, as well as maintenance on the motor, pump and pivot, estimated at $\$11.67 ha^{-1} cm^{-1}$ ($12.00/acre-inch) in Shurley and Smith (2013) and $\$9.48/ha^{-1}cm^{-1}$ ($9.75/acre-inch) in Shurley and Smith (2015). The cost equation is provided in equation 10, where *Irrig* was 0.254 cm per event (0.10 inch/event) and the $VarCost_{irrig}$ was $\$11.67\ ha^{-1}cm^{-1}$ ($12.00/acre-inch) in 2013 and $\$9.48\ ha^{-1}cm^{-1}$ ($9.75/acre-inch) in 2015, there was no budget available for 2014. Costs were estimated based upon 2013 and 2015 budgets.

$$Cost_{event} = Irrig * VarCost_{irrig} \quad (10)$$

RESULTS

All model results were verified using observed hourly canopy temperature data recorded at SIRP during 2013 and 2014 as mentioned previously in Methods.

Brown and Zeiher Model

R-squared values measuring the fit for the daytime and nighttime models are given in Table 2. Values improve substantially from 2013 and 2014. This may be due to the unusually wet growing season of 2013, which led to below normal temperatures in southwest Georgia. By contrast, the 2014 growing season was warmer and drier, which made the environment more similar to conditions in Arizona. Additionally, the Brown and Zeiher Model consistently underestimated canopy temperatures at SIRP during both the daytime and nighttime hours in

2013 and 2014. Theoretically, this may be due to the difference in mean vapor pressures between the Arizona site (where the model was developed) and the Georgia site. The humidity often encountered in the southeastern United States is higher, thus restricting plant cooling and likely resulting in lower modeled canopy temperatures than observed.

The Daytime and Nighttime Georgia Models

As discussed above, the Brown and Zeiher Model exhibited a large difference in performance between 2013 and 2014. This difference provided the motivation for developing a model specifically for Georgia. According to data from the National Climatic Data Center (NCDC, http://www.ncdc.noaa.gov), year-to-year variability in temperature and precipitation is common for the region, with some years recording mean temperatures greater than 28˚C while others average less than 25˚C. A robust canopy temperature model should be able to perform well within this range of observed variability.

The Daytime and Nighttime Georgia Models were developed using data from 2013 and verified using 2014 data. The P-values for the intercept and variable coefficients are listed in Table 3 and were less than 0.05, indicating they were statistically significant for both the daytime and nighttime models (referred to as the Daytime Georgia Model and Nighttime Georgia Model, respectively) at a 95% confidence level. Therefore, the intercept and all statistically significant variables were included in the model. The R^2 values are included in Table 2 and indicate better fits than the Brown and Zeiher model for both the daytime and nighttime periods during 2013 and 2014. Additionally, there was very little difference in R^2 values between 2013 and 2014 among the Daytime and Nighttime Georgia Models.

The 24-hour Georgia Model

The Daytime and Nighttime Georgia Models showed improvement over the results of the Brown and Zeiher Model. Noting it would be more convenient to have a model that represents the complete diurnal cycle, the 24-hour Georgia Model was developed with the addition of two variables (wind and solar radiation) using data from 2013. The P-values for the intercept and equation coefficients are provided in Table 3 and were all statistically significant at a 95% confidence interval.

Figures 1.a) through d) show different plots of the residuals and demonstrate that they resemble a normal distribution, have approximately constant variance, and display no correlation between error size and time, suggesting that the assumptions of linear regression hold thus justifying the use of linear regression to develop the model. The R^2 values are provided in Table 2 and indicate a better fit than the previous sets of models for the 2013 and 2014 seasons. There is slight skewing reflected in the histogram and normal probability plot, however, not enough to indicate the residuals are from a different type of distribution. Further analysis of outliers indicated that the largest residual values were generated when temperature and solar radiation values changed abruptly between hours, most likely indicating a sharp change in cloudiness. Although temperatures were below normal during the 2013 season, the Georgia Model does well fitting the approximately normal and climatologically different 2014 season. The 24-hour Georgia Model was chosen to simulate canopy temperature in this study due to its ease of applicability (one model used for both daytime and nighttime periods) as well as its ability to

model canopy temperature well over two climatologically very different years (NCDC, http://www.ncdc.noaa.gov).

Forecast Analysis

This section analyzes and compares the Direct Model Output (DMO) to the bias-corrected canopy temperature forecasts for 2014 alone considering bias corrections were developed from the 2013 forecasts. A popular way to verify and analyze weather forecasts is through the use of contingency tables (Nurmi 2003). Contingency tables separate forecasts into four distinct categories as shown in Table 4: hits (a), false alarms (b), misses (c), and correct rejections (d). The forecasts used in this experiment were converted into simple binary (or yes/no) forecasts using set probability thresholds. Each contingency table had a set probability threshold. Forecasts were grouped into the "yes" category if they exceeded the threshold (Christ et al. 2015). The highest probability of heat stress occurring during the 24-hour time period was selected as the probability to represent the heat stress forecast for the given day. Contingency tables were created for 2014 from forecast probability thresholds set from 0-100% for the unadjusted DMO as well as for the bias-corrected forecasts.

Relative Operating Characteristic (ROC) diagrams have become a common way to measure forecast performance (Nurmi 2003) as described in Figure 2. ROC diagrams were created from the contingency tables developed from the 2014 season by plotting the Hit Rate vs the False Alarm Rate. Equations for the Hit Rate and False Alarm Rate are provided in 11 and 12, respectively.

$$H = a/(a+c) \quad (11)$$

$$F = b/(b+d) \quad (12)$$

Where H is the Hit Rate, F is the False Alarm Rate, and a, b, c and d are defined in Table 4. The ROC diagrams are presented in Figs. 2.a) and 2.b). The diagrams and corresponding ROC areas confirm that both the forecasts for the unadjusted DMO and the bias-corrected forecasts were skillful out to day 10, although the bias-corrected forecasts were more skillful as indicated by higher ROC_a's across all lead days.

Besides ROC diagrams, several well-known performance measures can be calculated from contingency tables, among them Correct Warning (CWs) and Missed Events (MEs). CWs occurred when heat stress was observed and the forecast probability was equal to or exceeded a decision threshold. The relationship is provided in equation 13.

$$CW = a/(a+b) \quad (13)$$

Where CW is the probability that an event will occur given a warning is issued, and variables a and b are defined in Table 4. For example, if a producer decided to protect against heat stress only when the forecast probability of heat stress exceeded 70%, then a CW occurred when the forecast probability of heat stress was greater than or equal to 70% and heat stress was observed. The higher the probability of CW's at a given threshold, the better the forecast performed with respect to this parameter. Figures 3.a) and 3.b) show CWs for the unadjusted

DMO and bias-corrected 2014 forecasts, respectively. CWs were high for both categories and generally trended upward as forecast probability increased.

MEs occurred when heat stress was observed and the forecast probability was less than a set decision threshold. The relationship is provided in equation 14.

$$ME = c/(a+c) \tag{14}$$

Where ME is the probability that an event will occur given that no warning is issued. Variables a and c are defined in Table 4. For example, as above, if a producer's decision probability threshold was set at 70%, then a ME occurred when heat stress was observed and the forecast probability was less than 70%. A high rate of MEs would be particularly worrisome for producers who anticipate losses each time heat stress is observed and no action is taken to protect crops. For this application, it is important that forecasts minimize MEs. Figures 4.a) and 4.b) show MEs for the unadjusted DMO and bias-corrected 2014 forecasts, respectively. The number of MEs overall for the bias-corrected category was smaller than unadjusted DMO category, indicating the bias-corrected forecasts were superior.

Heat Stress Warning System

Figures 5. a) and b) are examples of heat stress forecasts generated from the probabilistic canopy temperature forecasts developed in this study. These forecasts are designed to warn producers of possible upcoming heat stress events. Figure 5.a) represents an 8-day forecast beginning 21 Aug. 2014 (observations were not recorded during the last two days of the period,

therefore, reducing the plot to 8 days), and Fig. 5.b) the 24-hour forecast for 22 Aug. 2014. The 8-day forecast provides daily information concerning medium-term conditions, while the 24-hour forecast presents a more detailed look at each hour during a given day. The 8-day forecast indicates a possible decrease in probability for heat stress late in the period, while the 24-hour forecast appropriately warns when canopy temperatures exceed stress levels within the diurnal cycle.

Economic Impact

The following is an explanation of how probabilistic forecasts can be utilized to aid producers with financial decisions pertaining to weather-related risks. The analysis provides a way to determine at what forecast probability level a producer should choose to protect based upon risk of loss and cost of protection. Currently, there are few multiple-year studies involving the relationship among canopy temperature, heat stress and yield. Although the study by Brown (2001) was conducted in Arizona and new cultivars have been developed since its development, the report concentrated on the effects of heat stress related to canopy temperature and yield. Thus, the reason for using it in this illustration.

Risk was calculated for probability levels 0-100% as outlined in Methods, plotted with cost and provided in Figs. 6 and 7. In this illustration, it is evident from Figs. 6 and 7 that the cost to protect in July (during reproduction) is very small compared to the potential losses. Therefore, protecting at very small forecast probabilities works out to be economically responsible. However, the circumstances change somewhat during the August and September timeframes when the cost to protect is closer to risk. Using prices from 2013 (2015) and

assuming more conservative losses, one would only protect if the forecast probability were greater than 80% (70%).

DISCUSSION

The results of this study suggest that it is possible to model canopy temperature based upon air temp, vapor pressure, solar radiation, and wind speed, using a single model for the diurnal period in Georgia. The 24-hr Georgia Model may make it possible to analyze previous years with respect to heat stress and yield. In that sense, it could be used in conjunction with past yield and weather data to better estimate the impact of heat stress on cotton yield. Although the 24-hr Georgia Model fit observations well during the 2013 and 2014 seasons, it would be beneficial to further measure its performance in the coming seasons or using past data. Additionally, it would be advantageous to analyze it with respect to canopy temperature data from other locations in the southeastern United States and worldwide to determine if it can be used over a wider area.

Coupling the 24-hr Georgia Model with the ECMWF EPS created canopy temperature forecasts that were skillful up to 10 days in advance, making it possible to warn producers of upcoming heat stress events. The ECMWF EPS DMO was further improved using simple statistical mean bias corrections. If forecasts such as these became available to growers, the extended warning period before heat stress events would allow producers time to plan for protecting crops, thus, preventing damage and yield loss. Nonetheless, it would be valuable to measure the performance of the coupled canopy temperature-atmospheric model in multiple locations over multiple growing seasons to determine its skill over a broader range.

The example economic analysis suggests that if variable irrigation costs and cotton sale prices remain within the 2013-2015 price range, it is financially reasonable to protect at very low forecast probabilities during periods in which the plant is most susceptible to heat stress. Beyond those most susceptible periods, expected losses are lower and a producer is free to act more conservatively with respect to protection. In the future, it might be possible to use exogenously applied compounds to protect against heat stress. In that case, the economic analysis performed for this work could be easily adjusted to represent the cost of the spray application. If work is done to quantify the effects of heat stress on yield in the southeastern United States, then this analysis could be updated to include data directly from the region to more accurately estimate the economic impact. The techniques used in this work are adaptable to other regions and other crops. Therefore, similar developments would seem possible for cotton and other crops in different climatic zones.

ACKNOWLEDGMENTS

This research has been supported by Cotton, Inc. We are indebted to ECMWF for providing data to make this analysis possible. We wish to thank Kater Hake and Ed Barnes for comments on the project as well as those at Stripling Irrigation Research Park who completed the field work for this study.

REFERENCES

Bhalla, N. (2015). This Indian City Developed A Heat Action Plan To Protect Vulnerable Citizens Amid Brutal Temperatures. Huffington Post.

British Atmospheric Data Centre. (2015). "European Centre for Medium-Range Weather Forecasts atmospheric level types." Retrieved 29 Jan. 2015, 2015, from http://badc.nerc.ac.uk/data/ecmwf-op/levels.html.

Brown, P. (2001). Heat Stress and Cotton Yields in Arizona. Cotton: A College of Agriculture Report. J. Silvertooth. Tucson, Arizona, The University of Arizona.

Brown, P. W. and C. A. Zeiher (1998). A Model to Estimate Cotton Canopy Temperature in the Desert Southwest. Beltwide Cotton Conference, Memphis, TN.

Burke, J. J. (1990). "Variation Among Species in the Temperature-Dependence of the Reappearance of Variable Fluorescence Following Illumination." Plant Physiology **93**(2): 652-656.

Burke, J. J., J. R. Mahan and J. L. Hatfield (1988). "Crop-Specific Thermal Kinetic Windows in Relation to Wheat and Cotton Biomass Production." Agronomy Journal **80**(4): 553-556.

Centers for Disease Control and Prevention. (2006, 15 August 2006). "Frequently Asked Questions (FAQ) about Extreme Heat." Retrieved 23 April 2015, 2015, from http://emergency.cdc.gov/disasters/extremeheat/faq.asp.

Centers for Disease Control and Prevention. (2014). "Heat Stress." Retrieved 4/23/2015, 2015, from http://www.cdc.gov/niosh/topics/heatstress/.

Christ, E. H., P. J. Webster, G. D. Collins, V. E. Toma and S. A. Byrd (2015). "Using Precipitation Forecasts to Irrigate Cotton." The Journal of Cotton Science.

Danforth, C. M., E. Kalnay and T. Miyoshi (2007). "Estimating and correcting global weather model error." Monthly Weather Review **135**(2): 281-299.

Durai, V. R. and R. Bhradwaj (2014). "Evaluation of statistical bias correction methods for numerical weather prediction model forecasts of maximum and minimum temperatures." Natural Hazards **73**(3): 1229-1254.

Farahani, H., et al. (2012). Cotton Irrigation Management for Humid Regions, Cotton Incorporated.

Glahn, H. R. and D. A. Lowry (1972). "The use of Model Output Statistics (MOS) in Objective Weather Forecasting." Journal of Applied Meteorology **11**: 1203-1211.

Hake, K. and J. Silvertooth (1990). High Temperature Effects on Cotton. Physiology Today. **1**.

Hopson, T. M. and P. J. Webster (2010). "A 1-10-Day Ensemble Forecasting Scheme for the Major River Basins of Bangladesh: Forecasting Severe Floods of 2003-07." Journal of Hydrometeorology **11**(3): 618-641.

Idso, S. B., R. D. Jackson, P. J. Pinter, R. J. Reginato and J. L. Hatfield (1981). "Normalizing the Stress-Degree-Day Parameter for Environmental Variability." Agricultural Meteorology **24**(1): 45-55.

Knowlton, K., et al. (2014). "Development and Implementation of South Asia's First Heat-Health Action Plan in Ahmedabad (Gujarat, India)." International Journal of Environmental Research and Public Health **11**(4): 3473-3492.

Kovats, R. S. and S. Hajat (2008). Heat stress and public health: A critical review. Annual Review of Public Health. Palo Alto, Annual Reviews. **29:** 41-55.

Lokhande, S. and K.R. Reddy. 2014. Quantifying temperature effects on cotton reproductive efficiency and fiber quality. Agron. J. 106:1275-1282.

Mahan, J. R., J. J. Burke and K. A. Orzech (1990). "Thermal-Dependence of the Apparent-Km Of Glutathione Reductases from 3 Plant-Species." Plant Physiology **93**(2): 822-824.

Mahan, J. R. and D. R. Upchurch (1988). "Maintenance of Constant Leaf Temperature by Plants .1. Hypothesis Limited Homeothermy." Environmental and Experimental Botany **28**(4): 351-357.

Nurmi, P. (2003). Recommendations on the verification of local weather forecasts (at ECMWF Member States). Reading, England, European Centre for Medium Range Weather Forecasts.

Oosterhuis, D. M. and J. L. Snider (2011). High Temperature Stress on Floral Development and Yield of Cotton. Stress Physiology in Cotton. Cordova, TN, The Cotton Foundation. **7:** 1-24.

Persson, A. (2011). User guide to ECMWF forecast products. Reading, UK, ECMWF.

Pettigrew, W.T. 2008. The effect of higher temperatures on cotton lint yield production and fiber quality. Crop Sci. 48:278-285.

Reddy, K.R., G.H. Davidonis, A.S. Johnson, B.T. Vinyard. 1999. Temperature regime and carbon dioxide enrichment alter cotton boll development and fiber properties. Agron. J. 91:851-858.

Shrestha, K. Y., P. J. Webster and V. E. Toma (2014). "An Atmospheric-Hydrologic Forecasting Scheme for the Indus River Basin." Journal of Hydrometeorology **15**(2): 861-890.

Shurley, D. and A. Smith (2013). 2013 Cotton Budgets, The University of Georgia

Shurley, D. and A. Smith (2015). 2015 Cotton Enterprise Budgets, University of Georgia.

Snider, J. L., D. R. Chastain, G. D. Collins, T. L. Grey and R. B. Sorensen (2015). "Do genotypic differences in thermotolerance plasticity correspond with water-induced differences in yield and photosynthetic stability for field-grown upland cotton?" Environmental and Experimental Botany **118**: 49-55.

Snider, J.L. and D.M. Oosterhuis. 2015. Physiology. In: D. Fang and R. Percy (eds) Agronomy Monograph 57, Cotton 2nd Edition. ASA-CSSA-SSSA, Madison, WI, pp 339-400.

Snider, J.L. and D.M. Oosterhuis. 2011. How does timing, duration, and severity of heat stress influence pollen-pistil interactions in angiosperms? Plant Signal. Behav. 6:930-933.

Snider, J.L. and D.M. Oosterhuis. 2012. Heat stress and pollen–pistil interactions. In: D.M. Oosterhuis and J.T. Cothren, editors, Flowering and Fruiting in Cotton. The Cotton Foundation, Cordova, TN. p. 59-78.

Upchurch, D. R. and J. R. Mahan (1988). "Maintenance of Constant Leaf Temperature by Plants .2. Experimental-Observations in Cotton." Environmental and Experimental Botany **28**(4): 359-366.

Webster, P. J. and J. Jian (2011). "Environmental prediction, risk assessment and extreme events: adaptation strategies for the developing world." Philosophical Transactions of the Royal Society a-Mathematical Physical and Engineering Sciences **369**(1956): 4768-4797.

Zhao, D., K.R. Reddy, V.G. Kakani, S. Koti, and W. Gao. 2005. Physiological causes of cotton fruit abscission under conditions of high temperature and enhanced ultraviolet-B radiation. Physiol. Plant. 124:189-199.

FIGURE CAPTION LIST

Fig. 1. a) Histogram, b) case order plot, c) normal probability plot, and d) residuals vs fitted values for the 24-hour Georgia Model. The plots suggest the assumptions of linear regression hold and justify developing the model using linear regression.

Fig. 2. a) 2014 unadjusted Direct Model Output (DMO) and b) 2014 Bias-Corrected Relative Operating Characteristic (ROC) diagrams. ROC diagrams are plots of the Hit Rate (a measure of the proportion of observed events that were correctly forecast) vs the False Alarm Rate (a measure of the proportion of forecast events that were incorrectly forecast). The closest points to the upper left hand corner of the plot represent the best forecasts. A measure of forecast performance derived from ROC diagrams is the ROC area (ROC_a). It is essentially the area under the curve. In a perfect system, the ROC_a is equal to 1, while a ROC_a less than 0.5 is considered unskillful.

Fig. 3. a) 2014 unadjusted Direct Model Output (DMO) and b) 2014 bias-corrected Correct Warning (CW) Probability vs Heat Stress. The probability of Correct Warnings (CW's) remained high after applying mean bias corrections to the European Centre for Medium-Range Weather Forecasts (ECMWF) Ensemble Prediction System (EPS) DMO.

Fig. 4. a) 2014 unadjusted and b) 2014 bias-corrected Missed Event (ME) Probability vs Heat Stress. The probability of ME's dropped after applying mean bias corrections to the European

Centre for Medium-Range Weather Forecasts (ECMWF) Ensemble Prediction System (EPS) Direct Model Output (DMO).

Fig. 5. a) 8-Day Cotton Heat Stress Forecast beginning 21 Aug. 2014 and b) 24-Hr Cotton Heat Stress Forecast for 22 Aug. 2014 at Camilla, Georgia. Observations for two days at the end of the 10-day period beginning 21 Aug. 2014 were not recorded, therefore, observations and forecasts were not included in the plot. The pink line represents the cotton heat stress threshold defined by the thermal kinetic window (32˚C). Observations above this line indicate heat stress. The black line represents observed canopy temperature. The multi-colored stems represent the heat stress forecast probability (length) and category (color) for the given day (Fig. 5. a) or hour (Fig. 5. b). Each stem color represents a probability range of exceeding 32˚C. Red stems indicate a 75% or greater probability, orange stems indicate between a 50% and 75% probability, yellow stems indicate between a 25% and 50% probability, and green stems indicate a 25% or less probability.

Fig. 6. a) 2013 and b) 2015 July Risk and Cost vs Forecast Probability. The cost of protection is very low compared to the risk of yield loss during the July time period when plants are most susceptible to heat stress.

Fig. 7. a) 2013 and b) 2015 Aug. and Sept. Risk and Cost vs Forecast Probability. Risk decreases later in the season when yield is less likely to be affected by heat stress.

TABLES

Table 1. Dates Excluded from Analysis. The dates listed were excluded due to pesticide applications or sensor failure.

Year	Month		
	July	***August***	***September***
2013	8, 10, 18-25	6-7, 14-17	---
2014	16, 19-22, 31	8-14, 29-30	1-8

Table 2. The R^2 values for canopy temperature models measured during 2013 and 2014. The R^2 value quantifies the nature and strength of a relationship between predictor (canopy temperature model) and predictand (measured canopy temperature). The closer the R^2 value to 1, the better the model fit the observed data.

Year	Model R^2 Value				
	Daytime Brown and Zeiher Model	***Daytime Georgia Model***	***Nighttime Brown and Zeiher Model***	***Nighttime Georgia Model***	***24-hr Georgia Model***
2013	0.73	0.89	0.40	0.87	0.94
2014	0.80	0.88	0.83	0.88	0.93

Table 3. P-values for the Daytime Georgia Model, the Nighttime Georgia Model, and the 24-hour Georgia Model, developed from data recorded in 2013. P-values <0.05 are indicative of model components that have a statistically significant effect upon the model fit at a 95% confidence level. All components listed below were statistically significant.

Models	**P-Values**					
	Intercept	***T_a***	***e_a***	***VPD***	***U***	***S***
Daytime Georgia Model	1.9E -03	3.69E-85	N/A	2.77E-08	N/A	N/A
Nighttime Georgia Model	7.21E -22	3.96E-129	2.09E-03	N/A	N/A	N/A
24-hr Georgia Model	4.35E -05	~ 0	1.36E -08	N/A	1.61E -15	1.08E -11

Table 4. A 2-X-2 Contingency Table. Contingency tables separate forecasts into four distinct categories (a-d). The variables generated from these categories are used to evaluate forecast performance.

	Event Observed		
Event Forecast	***Yes***	***No***	**Marginal Total**
Yes	a†	b‡	(a+b)§
No	c¶	d#	(c+d)††
Marginal Total	(a+c)‡‡	(b+d)§§	n = (a+b+c+d)¶¶

† referred to as a Hit

‡ referred to as a False Alarm

§ total number of times the event was forecast

¶ referred to as a Miss

referred to as a Correct Rejection

†† total number of times the event was not forecast

‡‡ total number of times the event was observed

§§ total number of time the event was not observed

¶¶ total number of forecasts in the season

FIGURES

Fig. 1. a) Histogram, b) case order plot, c) normal probability plot, and d) residuals vs fitted values for the 24-hour Georgia Model. The plots suggest the assumptions of linear regression hold and justify developing the model using linear regression.

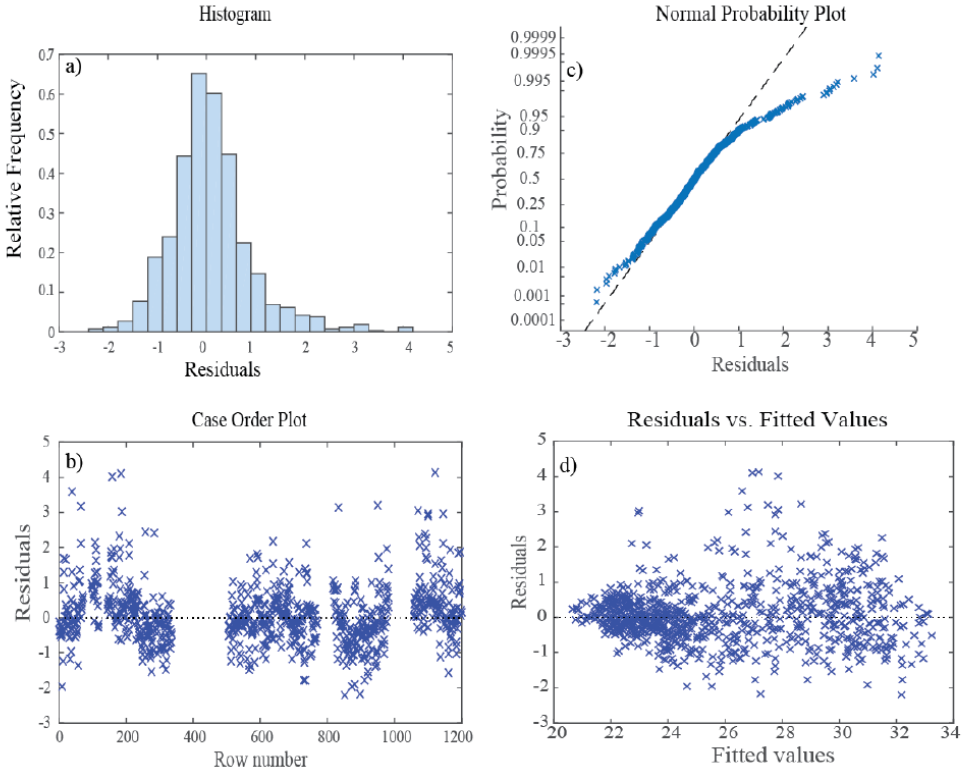

Fig. 2. a) 2014 unadjusted Direct Model Output (DMO) and b) 2014 Bias-Corrected Relative Operating Characteristic (ROC) diagrams. ROC diagrams are plots of the Hit Rate (a measure of the proportion of observed events that were correctly forecast) vs the False Alarm Rate (a measure of the proportion of forecast events that were incorrectly forecast). The closest points to the upper left hand corner of the plot represent the best forecasts. A measure of forecast performance derived from ROC diagrams is the ROC area (ROC_a). It is essentially the area under the curve. In a perfect system, the ROC_a is equal to 1, while a ROC_a less than 0.5 is considered unskillful. In the legend, LD = lead day. ROC_a's are calculated for each forecast lead day.

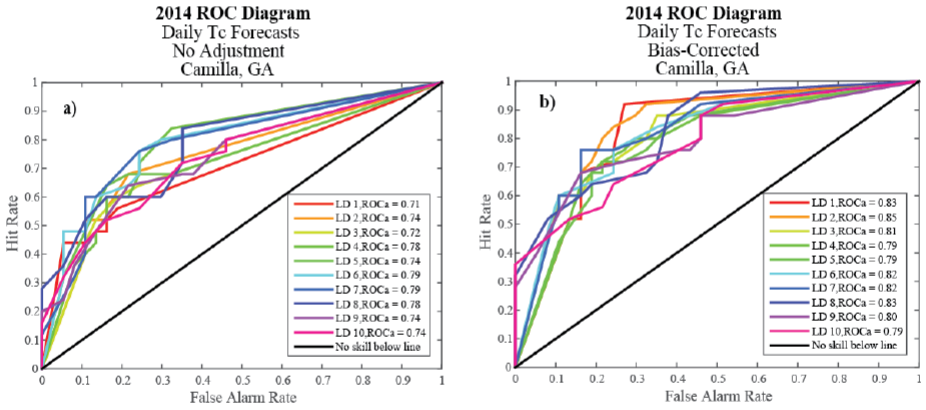

Fig. 3. a) 2014 unadjusted Direct Model Output (DMO) and b) 2014 bias-corrected Correct Warning (CW) Probability vs Heat Stress. The probability of CW's remained high after applying mean bias corrections to the European Centre for Medium-Range Weather Forecasts (ECMWF) Ensemble Prediction System (EPS) DMO.

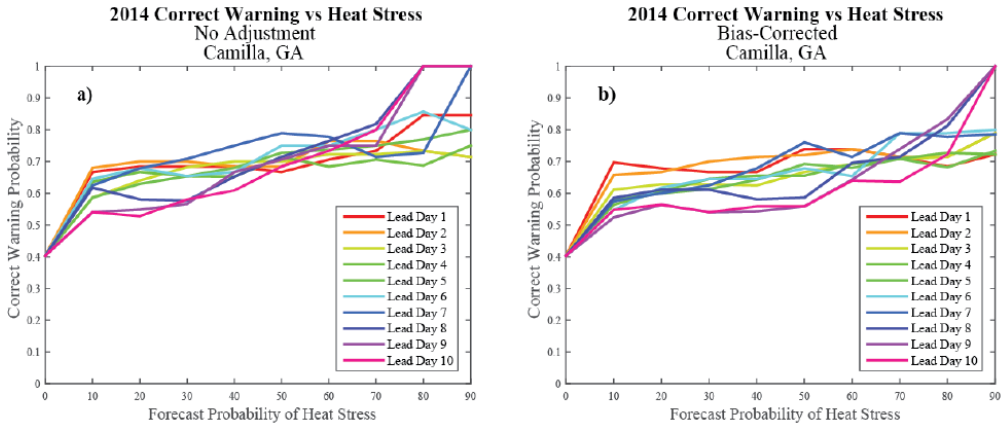

Fig. 4. a) 2014 unadjusted and b) 2014 bias-corrected Missed Event (ME) Probability vs Heat Stress. The probability of ME's dropped after applying mean bias corrections to the European Centre for Medium-Range Weather Forecasts (ECMWF) Ensemble Prediction System (EPS) Direct Model Output (DMO).

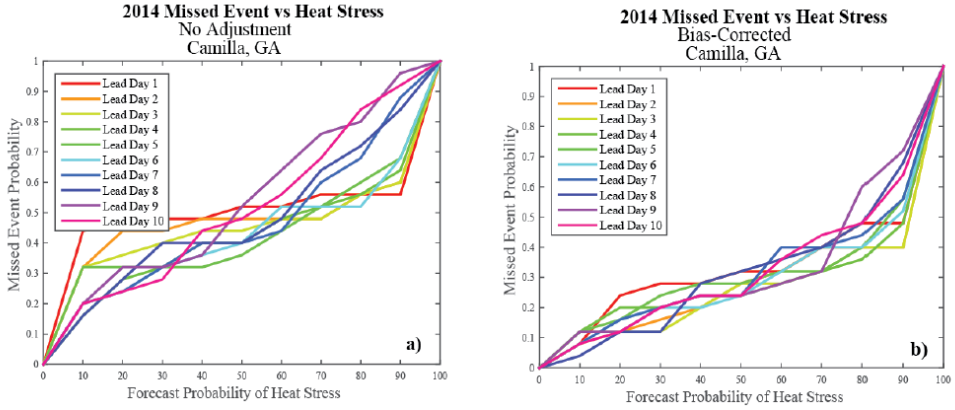

Fig. 5. a) 8-Day Cotton Heat Stress Forecast beginning 21 Aug. 2014 and b) 24-Hr Cotton Heat Stress Forecast for 22 Aug. 2014 at Camilla, Georgia. Observations for two days at the end of the 10-day period beginning 21 Aug. 2014 were not recorded, therefore, observations and forecasts were not included in the plot. The pink line represents the cotton heat stress threshold defined by the thermal kinetic window (32˚C). Observations above this line indicate heat stress. The black line represents observed canopy temperature. The multi-colored stems represent the heat stress forecast probability (length) and category (color) for the given day (Fig. 5. a) or hour (Fig. 5. b). Each stem color represents a probability range of exceeding 32˚C. Red stems indicate a 75% or greater probability, orange stems indicate between a 50% and 75% probability, yellow stems indicate between a 25% and 50% probability, and green stems indicate a 25% or less probability.

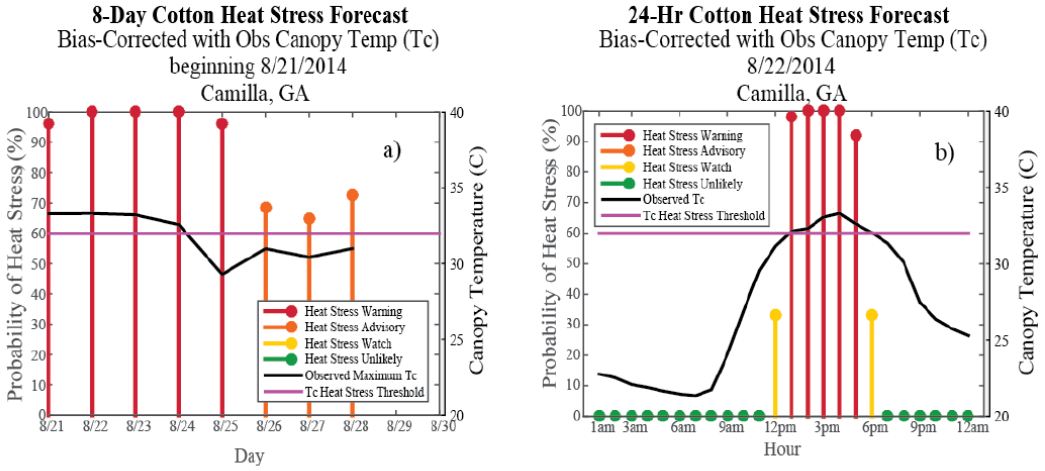

Fig. 6. a) 2013 and b) 2015 July Risk and Cost vs Forecast Probability. The cost of protection is very low compared to the risk of yield loss during the July time period when plants are most susceptible to heat stress.

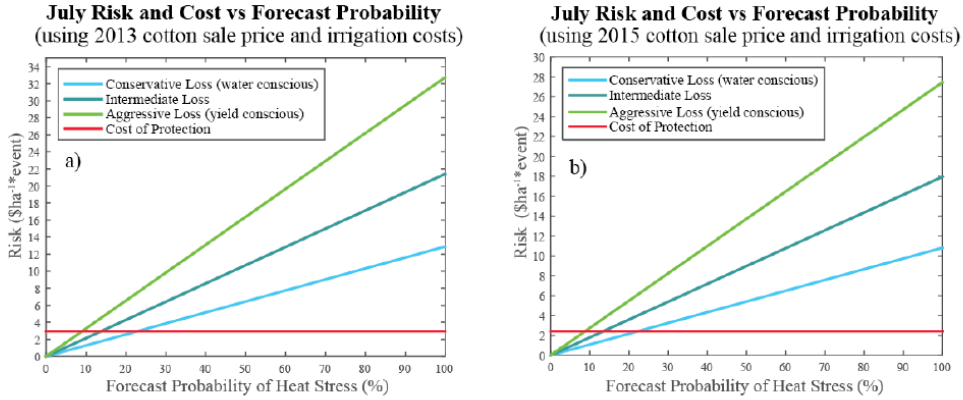

Fig. 7. a) 2013 and b) 2015 Aug. and Sept. Risk and Cost vs Forecast Probability. Risk decreases later in the season when yield is less likely to be affected by heat stress.

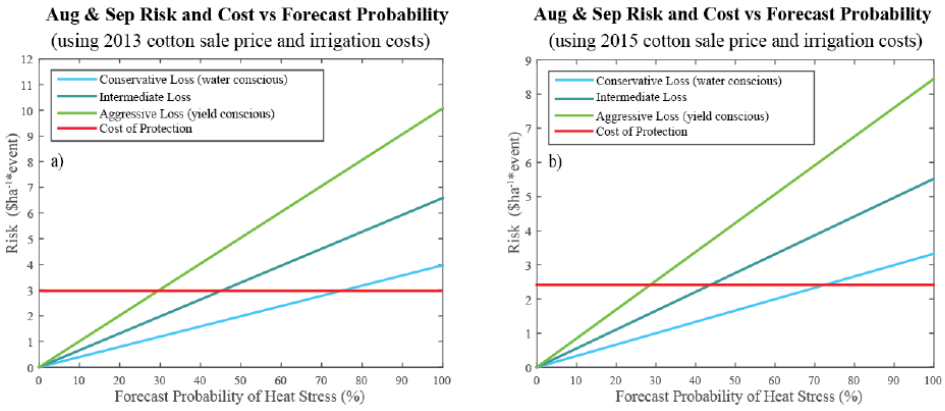

REFERENCES

Baigorria, G. A., J. W. Hansen, N. Ward, J. W. Jones, and J. J. O'Brien, 2008: Assessing predictability of cotton yields in the southeastern United States based on regional atmospheric circulation and surface temperatures. J. Appl. Meteor. Climatol. **47:** 76-91, doi: 10.1175/2007jamc1523.1.

Bhalla, N., 2015: This Indian City Developed A Heat Action Plan To Protect Vulnerable Citizens Amid Brutal Temperatures. Huffington Post. 28 May 2015.

British Atmospheric Data Centre. 2015: European Centre for Medium-Range Weather Forecasts atmospheric level types [Online]. Available at http://badc.nerc.ac.uk/data/ecmwf-op/levels.html. (verified 24 Sep. 2015).

Brown, P., 2001: Heat Stress and Cotton Yields in Arizona. Cotton: A College of Agriculture Report. J. Silvertooth. Tucson, Arizona, The University of Arizona.

Brown, P. W., and C. A. Zeiher, 1998: A Model to Estimate Cotton Canopy Temperature in the Desert Southwest. Beltwide Cotton Conference, Memphis, TN, 2:1734.

Burke, J. J., 1990: Variation Among Species in the Temperature-Dependence of the Reappearance of Variable Fluorescence Following Illumination. Plant Physiology. **93:** 652-656, doi: 10.1104/pp.93.2.652.

Burke, J. J., J. R. Mahan, and J. L. Hatfield, 1988: Crop-Specific Thermal Kinetic Windows in Relation to Wheat and Cotton Biomass Production. Agron. J. **80:** 553-556.

Centers for Disease Control and Prevention, 2015: Frequently Asked Questions (FAQ) about Extreme Heat. [Online] Available at http://emergency.cdc.gov/disasters/extremeheat/faq.asp. (verified 28 Jan. 2016).

Center for Disease Control and Prevention, 2015. Heat Stress. [Online] Available at http://www.cdc.gov/niosh/topics/heatstress/. (verified 28 Jan. 2016).

Christ, E. H., P. J. Webster, G. D. Collins, V. E. Toma, and S. A. Byrd, 2015a: Using Precipitation Forecasts to Irrigate Cotton. J. Cotton Sci. 19(3):351-358.

Christ, E. H., P. J. Webster, J. L. Snider, V. E. Toma, D. M. Oosterhuis, and D. R. Chastain, 2015b: Predicting Heat Stress in Cotton Using Probabilistic Canopy Temperature Forecasts. Agron. J. (Submitted).

Crane, T. A., C. Roncoli, J. Paz, N. Breuer, K. Broad, K. T. Ingram, and G. Hoogenboom, 2010: Forecast skill and farmers' skills: Seasonal climate forecasts and agricultural risk management in the southeastern United States. Weather Climate and Society. **2:** 44-59, doi: 10.1175/2010wcas1075.1.

Danforth, C. M., E. Kalnay, and T. Miyoshi, 2007: Estimating and correcting global weather model error. Mon. Wea. Rev. **135:** 281-299, doi: 10.1175/mwr3289.1.

Durai, V. R., and R. Bhradwaj, 2014: Evaluation of statistical bias correction methods for numerical weather prediction model forecasts of maximum and minimum temperatures. Natural Hazards. **73:** 1229-1254, doi: 10.1007/s11069-014-1136-1.

Farahani, H., and D. Munk, 2012: Why irrigate cotton? p. 2-6 *In* C. Perry and E. Barnes, (ed.), Cotton Irrigation Management for Humid Regions, Cotton, Incorporated, Cary, NC.

Farahani, H., et al., 2012: Cotton Irrigation Management for Humid Regions. C. Perry and E. Barnes, (ed.), Cotton Incorporated, Cary, NC.

Glahn, H. R., and D. A. Lowry, 1972: The use of Model Output Statistics (MOS) in Objective Weather Forecasting. Journal of Applied Meteorology. **11:**1203-1211.

Hake, K., and J. Silvertooth, 1990: High Temperature Effects on Cotton. Physiology Today. **1(10)**.

Hansen, J. W., A. W. Hodges, and J. W. Jones, 1998: ENSO influences on agriculture in the southeastern United States. J. Climate. **11:** 404-411, doi: 10.1175/1520-0442(1998)011<0404:eioait>2.0.co;2.

Hansen, J. W., J. W. Jones, A. Irmak, and F. Royce, 2001: El Nino-Southern Oscillation impacts on crop production in the southeast United States. p. 57-78 *In* J. L. Hatfield et al. (eds.), Impacts of El Nino and Climate Variability on Agriculture. American Society of Agronomy, Madison, WI.

Hollis, P., 2013: Irrigation scheduling tools seen as a key to conserving water in southwest Georgia. Southeast Farm Press [Online]. Available at http://southeastfarmpress.com/equipment/irrigation-scheduling-tools-seen-keyconserving-water-southwest-georgia (verified 17 Sep.2015).

Hoogenboom, G., J.W. Jones, P.W. Wilkens, C.H. Porter, K.J. Boote, L.A. Hunt, U. Singh, J.I. Lizaso, J.W. White, O. Uryasev, R. Ogoshi, J. Koo, V. Shelia, and G.Y. Tsuji., 2015. Decision Support System for Agrotechnology Transfer (DSSAT) Version 4.6 (www.DSSAT.net). DSSAT Foundation, Prosser, Washington.

Hopson, T. M., and P. J. Webster, 2010: A 1-10-Day Ensemble Forecasting Scheme for the Major River Basins of Bangladesh: Forecasting Severe Floods of 2003-07. J. Hydrometeorology. **11:**618-641, doi: 10.1175/2009jhm1006.1.

Idso, S. B., R. D. Jackson, P. J. Pinter, R. J. Reginato, and J. L. Hatfield, 1981: Normalizing the Stress-Degree-Day Parameter for Environmental Variability. Agricultural Meteorology. **24:**45-55, doi: 10.1016/0002-1571(81)90032-7.

Jones, J.W., G. Hoogenboom, C.H. Porter, K.J. Boote, W.D. Batchelor, L.A. Hunt, P.W. Wilkens, U. Singh, A.J. Gijsman, and J.T. Ritchie, 2003. DSSAT Cropping System Model. European Journal of Agronomy **18:**235-265.

Knowlton, K., et al., 2014: Development and Implementation of South Asia's First Heat-Health Action Plan in Ahmedabad (Gujarat, India). International Journal of Environmental Research and Public Health. **11:** 3473-3492, doi: 10.3390/ijerph110403473.

Kovats, R. S., and S. Hajat, 2008: Heat stress and public health: A critical review. Annu. Rev. of Public Health. **29:**41-**55**.

Leib, B., G. Sassenrath, and A. M. Schmidt, 2012: Irrigation scheduling tools. p. 32-37 *In* C. Perry, and E. Barnes, (eds.), Cotton Irrigation Management for Humid Regions. Cotton, Incorporated, Cary, NC.

Mahan, J. R., and D. R. Upchurch, 1988: Maintenance of Constant Leaf Temperature by Plants .1. Hypothesis Limited Homeothermy. Environmental and Experimental Botany. **28:** 351-357, doi: 10.1016/0098-8472(88)90059-7.

Mahan, J. R., J. J. Burke, and K. A. Orzech, 1990: Thermal-Dependence of the Apparent-Km of Glutathione Reductases from 3 Plant-Species. Plant Physiology. **93:** 822-824, doi: 10.1104/pp.93.2.822.

Nurmi, P. 2003. Recommendations on the verification of local weather forecasts (at ECMWF Member States). Series: ECMWF Technical Memoranda. European Centre for Medium-Range Weather Forecasts, Reading, England.

Oosterhuis, D. M., and J. L. Snider, 2011: High Temperature Stress on Floral Development and Yield of Cotton. p. 1-24 *In* D.M. Oosterhuis (ed.), Stress Physiology in Cotton. The Cotton Foundation, Cordova, TN.

Ortiz, B. V., G. Hoogenboom, G. Vellidis, K. Boote, R. F. Davis, and C. Perry, 2009: Adapting the Cropgro-Cotton Model to Simulate Cotton Biomass and Yield Under Southern Root-Knot Nematode Parasitism. Transactions of the ASABE, **52:** 2129-2140.

Paz, J. O., P. Woli, A. Garcia Y Garcia, and G. Hoogenboom, 2012: Cotton yields as influenced by ENSO at different planting dates and spatial aggregation levels. Agricultural Systems. **111:** 45-52, doi: 10.1016/j.agsy.2012.05.004.

Persson, A., 2011: User guide to ECMWF forecast products. European Centre for Medium-Range Weather Forecasts, Reading, UK.

Pfister, S., P. Bayer, A. Koehler, and S. Hellweg, 2011: Projected water consumption in future global agriculture: Scenarios and related impacts. Sci. Total Environ. **409:** 4206-4216, doi: 10.1016/j.scitotenv.2011.07.019.

Shrestha, K. Y., P. J. Webster, and V. E. Toma, 2014: An Atmospheric-Hydrologic Forecasting Scheme for the Indus River Basin. J. Hydrometeorology. **15:** 861-890, doi: 10.1175/jhm-d-13-051.1.

Shurley, D., and A. Smith, 2013: 2013 Cotton Budgets. The University of Georgia College Agricultural and Environmental Sciences [Online]. Available at http://www.caes.uga.edu/departments/agecon/extension/budgets/cotton/index.html. (verified 28 Jan. 2016).

Shurley, D., and A. Smith, 2015: 2015 Cotton Enterprise Budgets. The University of Georgia College Agricultural and Environmental Sciences [Online]. Available at http://www.caes.uga.edu/departments/agecon/extension/budgets/cotton/index.html. (verified 28 Jan. 2016).

Snider, J. L., D. R. Chastain, G. D. Coillins, T. L. Grey, and R. B. Sorensen, 2015: Do genotypic differences in thermotolerance plasticity correspond with water-induced differences in yield and photosynthetic stability for field-grown upland cotton? Environmental and Experimental Botany. **118:** 49-55, doi: 10.1016/j.envexpbot.2015.06.005.

Tiedtke, M., 1989: A Comprehensive mass flux scheme for cumulus parameterization in large-scale models. Mon. Wea. Rev. **117:** 1779-1800, doi: 10.1175/1520-0493(1989)117<1779:acmfsf>2.0.co;2.

Tilman, D., C. Balzer, J. Hill, and B. L. Befort, 2011: Global food demand and the sustainable intensification of agriculture. Proceedings of the National Academy of Sciences of the United States of America. **108:** 20260-20264, doi: 10.1073/pnas.1116437108.

UN Dept of Economic and Social Affairs, 2004: World Population to 2300. United Nations, United Nations, NY.

University of Georgia Cooperative Extension/ College of Agricultural and Environmental Sciences, 2014: 2014 Georgia cotton production guide. Cooperative Extension Service/University of Georgia, Tifton, GA

Upchurch, D. R., and J. R. Mahan, 1988: Maintenance of Constant Leaf Temperature by Plants .2. Experimental-Observations in Cotton. Environmental and Experimental Botany. **28:** 359-366, doi: 10.1016/0098-8472(88)90060-3.

VITA

EMILY HALL CHRIST

CHRIST was born in Florence, Alabama. She attended West Limestone High School in Lester, Alabama, received a B.S. in Chemical Engineering from the University of Alabama in Huntsville, Huntsville, Alabama in 2002 and a M.S. in Civil and Environmental Engineering from the University of Alabama in Huntsville, Huntsville, Alabama in 2005. She worked as an environmental engineering consultant for four years and became a licensed Professional Engineer in Alabama and Georgia before coming to Georgia Tech to pursue a doctorate in Dynamics of Weather and Climate at the School of Earth and Atmospheric Sciences.